

**A STUDY OF THE LAWS OF THE FLOW OF FLUIDS
THROUGH FABRICS**

CECIL D. BROWN

GEORGIA INSTITUTE OF TECHNOLOGY

JANUARY 1955

MATERIALS LABORATORY
CONTRACT No. AF 33(038)-15624
PROJECT No. 7320

WRIGHT AIR DEVELOPMENT CENTER
AIR RESEARCH AND DEVELOPMENT COMMAND
UNITED STATES AIR FORCE
WRIGHT-PATTERSON AIR FORCE BASE, OHIO

Contrails

FOREWORD

This report was prepared by the Georgia Institute of Technology under USAF Contract No. AF 33(038)-15624. The contract was initiated under Project No. 7320, "Air Force Textile Materials", Task No. 73201, "Textile Materials for Parachutes", formerly RDO No. 612-12, "Textiles for High Speed Parachutes", and was administered under the direction of the Materials Laboratory, Directorate of Research, Wright Air Development Center, with Mr. Jack H. Ross acting as project engineer.

WADC TR 54-199

Contrails

ABSTRACT

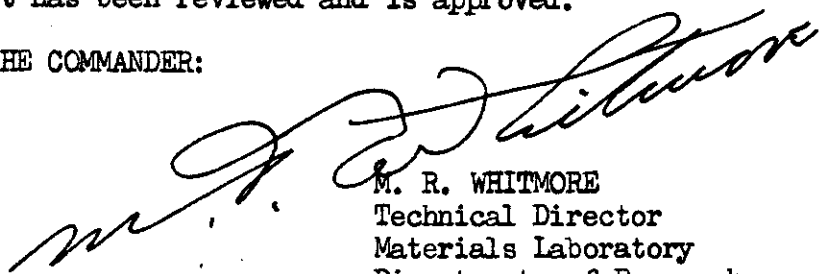
In this study a method is developed of presenting the flow data in a general dimensionless form over a limited range of flow. Under the assumption that the pressure-squared gradient in the flow through a fabric is the arithmetic sum of the viscous ($2\alpha RT \frac{\Delta G}{g_c}$) and the inertial contributions ($2\beta \frac{RT}{g_c} G^2$), it is possible to infer the existence of a characteristic length L . The relation between the flow-through-drag coefficient and the Reynolds number based on this characteristic length, $C_f = \frac{2}{N_{Re}} + 2$, is common to all fabrics. The parameters α and β and the characteristic length can be obtained from only two flow measurements.

The parameters α and β may be estimated from physical measurements of the cloth, thus permitting a rough prediction of the permeability of the fabric.

PUBLICATION REVIEW

This report has been reviewed and is approved.

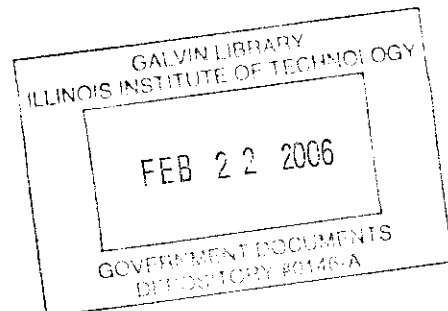
FOR THE COMMANDER:



M. R. WHITMORE
Technical Director
Materials Laboratory
Directorate of Research

WADC TR 54-199

iii



Contrails

TABLE OF CONTENTS

	Page
INTRODUCTION	1
A Brief History of the Problem	2
Objectives of This Work	6
THEORY	7
EXPERIMENTAL PROCEDURE	11
Apparatus	11
Test Procedure	19
Calculations	22
TEST RESULTS	23
PERMEABILITY PREDICTION STUDY	32
CONCLUSIONS	37
APPENDIX A--Summary of Results	39
APPENDIX B--Sample Calculations	61
NOMENCLATURE	72
BIBLIOGRAPHY	74

Contrails

LIST OF TABLES

<u>Table</u>	<u>Page</u>
1. Physical Properties of Bally Ribbon Cloths	39
2. Experimental Data for Fabric Number BR-1	40
3. Experimental Data for Fabric Number BR-2	41
4. Experimental Data for Fabric Number BR-5	42
5. Experimental Data for Fabric Number BR-6	43
6. Experimental Data for Fabric Number BR-9	44
7. Experimental Data for Fabric Number BR-10	45
8. Experimental Data for Fabric Number BR-11	46
9. Experimental Data for Fabric Number BR-12	47
10. Experimental Data for Fabric Number BR-13	48
11. Experimental Data for Fabric Number BR-14	49
12. Experimental Data for Fabric Number BR-17	50
13. Experimental Data for Fabric Number BR-18	51
14. Experimental Data for Fabric Number BR-30	52
15. Experimental Data for Fabric Number BR-40	53
16. Experimental Data for 100 Mesh Wire Screen	54
17. Experimental Data for 150 Mesh Wire Screen	55
18. Experimental Data for 200 Mesh Wire Screen	56
19. Experimental Data for 270 Mesh Wire Screen	57
20. α and β Values for Fabrics and Screens	58
21. Physical Dimensions of Fabrics	59

Continued
LIST OF TABLES (CONTINUED)

<u>Table</u>	<u>Page</u>
22. Physical Dimensions of Screens	60
23. Data on Averaged Pressure Drop versus Static Pressure	70
24. Sample Data and Result Sheet	71

Contrails

LIST OF ILLUSTRATIONS

<u>Figure</u>	<u>Page</u>
1. Test Setup	12
2. Gauge Board	13
3. Typical Orifice Installation	14
4. Exploded View of Sample Holder	16
5. Upstream Face of Sample Holder	17
6. Downstream Face of Sample Holder	18
7. Low-Pressure Tunnel	20
8. ψ versus Mass Velocity for Fabric BR-1	24
9. ψ versus Mass Velocity for Fabric BR-30	25
10. ψ versus Mass Velocity for Fabric BR-40	26
11. ψ versus Mass Velocity for 100 Mesh Screen	27
12. ψ versus Mass Velocity for 270 Mesh Screen	28
13. Relation of Flow-Through-Drag Coefficient to Reynolds Number	31
14. Relation of α to Fabric Geometry	34
15. Relation of β to Fabric Geometry	35
16. Master Data and Result Sheet	66
17. Orifice Coefficient Curve	67
18. Sample Log Sheet	68
19. Relation of Static Pressure to Orifice Pressure Drop	69

Contrails

Contrails

CHAPTER I

INTRODUCTION

During the past few years a steadily increasing interest has been taken in the laws governing the flow of fluids through fabrics, and many experimental and theoretical investigations have been made in order to determine the relationship existing between the many variables. There has been a greater demand for such knowledge due to the increasing variety of textile fibers available and to their wide range of uses. For instance, the army must furnish uniforms which will provide comfort and protection for the wearer in climates ranging from tropic to arctic, from jungle to desert. The Air Force is using parachutes for dropping entire armies, including their vehicles and heavy weapons. The designer of textile materials for such purposes must have a knowledge of all the properties of the fabric including its permeability. The comfort of the soldier will depend upon the proper circulation of air through his uniform; the stability and rate of descent of the parachute will depend upon the flow of air through the fabric of the canopy.

Although the terms "permeability" and "porosity" are often used interchangeably, in this paper permeability is defined as "the rate of flow of fluid under differential pressure through an area of material. The term "plane porosity" is defined as the ratio of the open area of the fabric to the total area. The term "fluid" refers to both liquids and gases.

Contrails

A brief history of the problem.--Investigations into the flow of fluids through fabrics have been carried out with four main objectives:

1. The development of instruments for the measurement of permeability.
2. The determination of the factors influencing the permeability of fabrics.
3. The prediction of fabric permeability from simple measurements of the cloth.
4. The determination of general laws governing such flow.

Instruments.--Although a wide variety of instruments have been developed for the measurement of the permeability of fabrics they all belong to one of three general groups.

To the first group belong those in which the permeability is determined by the time required for a measured volume of air under constant pressure to flow through a measured area of cloth. This type, which is exemplified by the Gurley Densometer (1), has the advantage of simplicity and ease of operation, but it is limited to one pressure differential and to a small sample area.

In the second class are those in which the air is drawn through the cloth, is measured by an inclined manometer and the rate of flow of air is measured by an orifice meter. The most widely used instrument of this type is the Frazier machine, which was designed for the U. S. Bureau of Standards and is described in detail by Schiefer and Boyland (2). One feature of this machine is that the pressure drop can be controlled by varying the speed of the suction fan. Another advantage is that the temperature and humidity of the entering air are the same as

Contrails

that of the air in the room.

In the third type of machine the air is blown through the cloth. In one variation the air is furnished directly by a blower or compressor. In another variation the air is supplied from a reservoir. The latter type has the advantage that the air can be conditioned in the storage tank, whereas it is usually impractical to control the temperature and humidity of air coming direct from a blower. The machines used in this work were of the blower type (see Chapter III).

Factors influencing fabric permeability.---The rate of flow of a fluid through a fabric under a given pressure differential is a function of the physical properties of the fluid and of the geometry of the cloth. The properties of the fluid which affect the flow are temperature, viscosity, and density. Other properties, such as humidity, are important only if they affect the physical properties of the fabric.

The geometry of the fabric is described by such things as the type of weave, thread spacing, size and twist of the threads, and the nature of the fibers (3). The geometry may have been changed after weaving by the finish given the cloth, and it may be changed during the test by such factors as tension, temperature, humidity, etc.

It has been determined empirically that, for a given texture, the plain weave has the lowest permeability and the satin the highest (4). The permeability has been found to decrease as the number of threads per inch or the size of the threads is increased. Increasing the twist given the yarns has the effect of increasing the permeability, apparently by keeping the individual fibers in a more compact bundle. The general effects of test conditions (tension, temperature, relative

Contrails

humidity, and time element) are described by Rainard (5).

Permeability predictions from fabric geometry.--In attempting to predict the air permeability from the geometry of the fabrics some workers have treated the open area of the cloth as a series of small nozzles. Robertson (6), after making a series of tests on a number of wire screens and open weave fabrics, calculated the discharge coefficient defined by the general flow equation:

$$K = \frac{Q}{A_2 \sqrt{1 - \left(\frac{A_2}{A_1}\right)^2} \sqrt{\Delta P}} \quad (1)$$

For screens he obtained fair agreement that the coefficient K is a function of only the Reynolds number, i.e., by plotting the discharge coefficient against the Reynolds number for the screens he obtained one curve. However, the fabrics gave poor correlation, even among those of the same type weave, but varying texture. Since it has been shown that, for a given texture, the permeability varies with the weave, and since the projected open area is independent of the weave, the best that could come from this type of presentation is a curve for each type of weave.

Backer (7) has proposed that the minimum pore area be used as the area of the nozzle instead of the projected open area. He states that all weaves are composed of a combination of four basic types of yarn intermesh which he describes as follows:

If planes perpendicular to the fabric surfaces and bisecting any two adjacent warp and filling yarns are used to form a unit cell, four basic categories of pores can be established: type I, in which all four yarns of the unit cell alternate from the top to the bottom

Contrails

surface of the cloth and vice versa; type II, in which one warp and one filling yarn alternate; type III in which no alternation of the yarns takes place; and type IV, in which either two warp yarns or two filling yarns alternate from top to bottom surface or vice versa.

The minimum pore area can be determined graphically by cutting the unit cell with a series of planes parallel to the plane of the fabric and of varying depth. It has been found that the type I pore has the smallest minimum cross-sectional area, while the type III interstice has the greatest. This is consistent with test results since the plain weaves of lower permeability consist entirely of type I cells, while the more permeable satins have a large per cent of type III pores.

The theory of a minimum pore area has had limited applications, partly due to the difficulty of calculating these areas. Robertson (8) applied it to a limited number of fabrics and screens, but did not obtain conclusive results.

Laws governing the flow of fluids through fabrics.--An examination of the literature shows no general law that will apply to a wide range of flows and pressure differentials. Darcy's law has been suggested, but its range of validity is for flows much lower than those of general interest. Landsbery and Winston (9) derived an empirical relationship between the permeability as given by the Frazier machine at 0.5 inches of water and the Gurley Densometer at 1.26 inches of water. Since it has no scientific basis this formula is of limited value.

Goglia (10) has proposed that a similarity exists between the flow through a fabric and the flow through a porous bed. The flow through the latter is given by the equation:

Contrails

$$-\frac{dp}{dx} = \alpha \mu v + \beta \rho v^2 \quad (2)$$

From which the Reynolds number can be determined as

$$N_{Re} = \frac{\beta \rho v}{\alpha \mu} \quad (3)$$

If the analogy does exist, the flow for any fabric can be completely described once the two parameters α and β are determined; furthermore, these parameters can be found by making only two observations at a high and a low flow. There is also the possibility that they can be obtained from the geometry of the fabric. Preliminary tests on a small group of fabrics indicate that the similarity does exist.

Objectives of this work.--The objectives of this work are to:

1. Evaluate the parameters α and β for a number of parachute fabrics.
2. Determine the range over which the proposed law is valid.
3. Develop a means of obtaining the parameters from simple measurements of the cloth.

THEORY

Since the interstice of the unit cell is of too complex a form to permit a complete analytical solution of the flow, investigators have attempted to find a similarity between the flow through fabrics and some other type of flow. The existence of some similarity between the flow through fabrics and through porous beds as proposed by Goglia (11) is shown by the general agreement that in both cases the viscous forces predominate for low values of the Reynolds number, while for high Reynolds numbers the inertia forces control. In neither case can the geometry of the system be characterized by only one measure of length. For both fabrics and porous beds there exists a wide intermediate range of flows in which neither set of forces predominate, there being no abrupt transition from laminar to turbulent flow such as occurs in flow in pipes.

Flow through porous beds.--Green and Duwez (12) argue that the transition from the viscous regime to the inertial regime is characterized by losses due to a linear combination of the viscous and inertial forces. For the flow of an incompressible fluid the pressure gradient can be expressed as:

$$-\frac{dp}{dx} = \alpha \mu v + \beta \rho v^2 \quad (4)$$

For isothermal flow of a gas through a porous bed the pressure-square

Contrails

gradient is:

$$\frac{P_1^2 - P_2^2}{L} = \alpha \left(2RT \frac{\mu}{g_c} \right) G + \beta \left(\frac{2RT}{g_c} \right) G^2 \quad (5)$$

The Reynolds number, which is defined as the ratio of the inertia forces to the viscous forces, becomes under this treatment

$$N_{Re} = \frac{\beta \rho V}{\alpha \mu} = \frac{\beta G}{\alpha \mu} \quad (6)$$

They further define a flow-through-resistance coefficient as

$$C_f = \frac{-\frac{dp}{dx}}{\frac{\beta \rho V^2}{2}} = \frac{\frac{\nabla P^2}{\beta L}}{RTG^2} \quad (7)$$

By combining equations (5) and (7) the resistance coefficient may be defined as

$$C_f = \frac{2}{N_{Re}} + 2 \quad (8)$$

In the equations (4) to (8) the viscous coefficient α has the dimension negative two in length (L^{-2}) and the inertia coefficient β has the dimension negative one in length (L^{-1}); both serve to characterize the structure of the porous material itself. Thus the ratio β / α may be seen to represent a "characteristic length" which will describe the geometry of the bed.

Limitations of this theory as applied to fabrics.--It should be noted that the equations were derived for a bed of fixed geometry, and that the parameters α and β are functions of the geometry of the beds. Thus,

Contrails

the equations can be applied to fabrics only under the assumptions that the deformation of the cloth is negligible, and that α and β are not functions of the velocity of flow.

There is also the likelihood that this law cannot hold for high Reynolds numbers in a flow through a lightweight fabric. For instance, if the ratio of the thread diameter to thread spacing is small, the flow may approximate the flow around a series of isolated cylinders. The drag-coefficient versus Reynolds-number curve for a cylinder certainly could not be defined by an equation of the type

$$C_f = \frac{2}{N_{Re}} + 2 \quad (8)$$

except for low Reynolds number.

Determination of the parameters α and β ---The parameters α and β can best be determined from the data if a new variable is defined as

$$\psi = \frac{\nabla P^2}{2RTG} \quad (9)$$

and the pressure-square gradient equation rewritten in the form

$$\psi = \frac{\nabla P^2}{2RTG} = \alpha \frac{L \mu}{g_c} + \frac{\beta L}{g_c} G \quad (10)$$

Thus, under the previous assumptions, the dependent variable ψ is a linear function of the independent variable G , and the flow agrees with the proposed law over the region for which the experimental data plot as a straight line. This is important since it gives a straight line relation for ψ and G on plain coordinate paper, even in the transition

Contrails

range. This type of presentation has a greater sensitivity to deviations of the experimental data from the empirical curve than does the presentation using logarithmic scales. Furthermore, for any particular temperature of the fluid, the constant $\alpha L \frac{\mu}{g_c}$ is the intersection of the curve and the y-axis; the slope of the curve is given by $\frac{\beta L}{g_c}$. Thus, the parameters α and β can be obtained from two values of ∇P and G .

EXPERIMENTAL PROCEDURE

Apparatus.--Two separate pieces of apparatus were used in this investigation in order to obtain a wide variation of flows. Both machines were designed and built at the State Engineering Experiment Station at Georgia Institute of Technology.

The high pressure apparatus.--The first piece of apparatus was designed to produce a high pressure differential across the cloth. It consists essentially of a motor driven blower, a wind tunnel containing an orifice meter, a sample holder, and instruments (Figs. 1 and 2).

The blower, which was built by the Buffalo Forge Company, is of the centrifugal type with a 28 inch rotor and is capable of producing a static pressure of 55 inches of water. It is powered by a 7 1/2 horse power electric motor. The volume of air entering the blower is controlled by a conical plug at the inlet (Fig.1).

The wind tunnel is ten feet long with an internal diameter of 5.75 inches. The transition section from the blower to the tunnel and one section of the tunnel are made of 16-gauge galvanized iron; the remainder of the tunnel is built of plexi-glass tubing. A flange-tap type orifice, installed in the tunnel in accordance with the specifications of the ASME Special Research Committee on Fluid Meters (12), is used to measure the rate of flow of air (Fig. 3). The sample holder is fastened to a flange built on the outlet end of the tunnel, thus, leaving the downstream face of the cloth subject to atmospheric pressure.

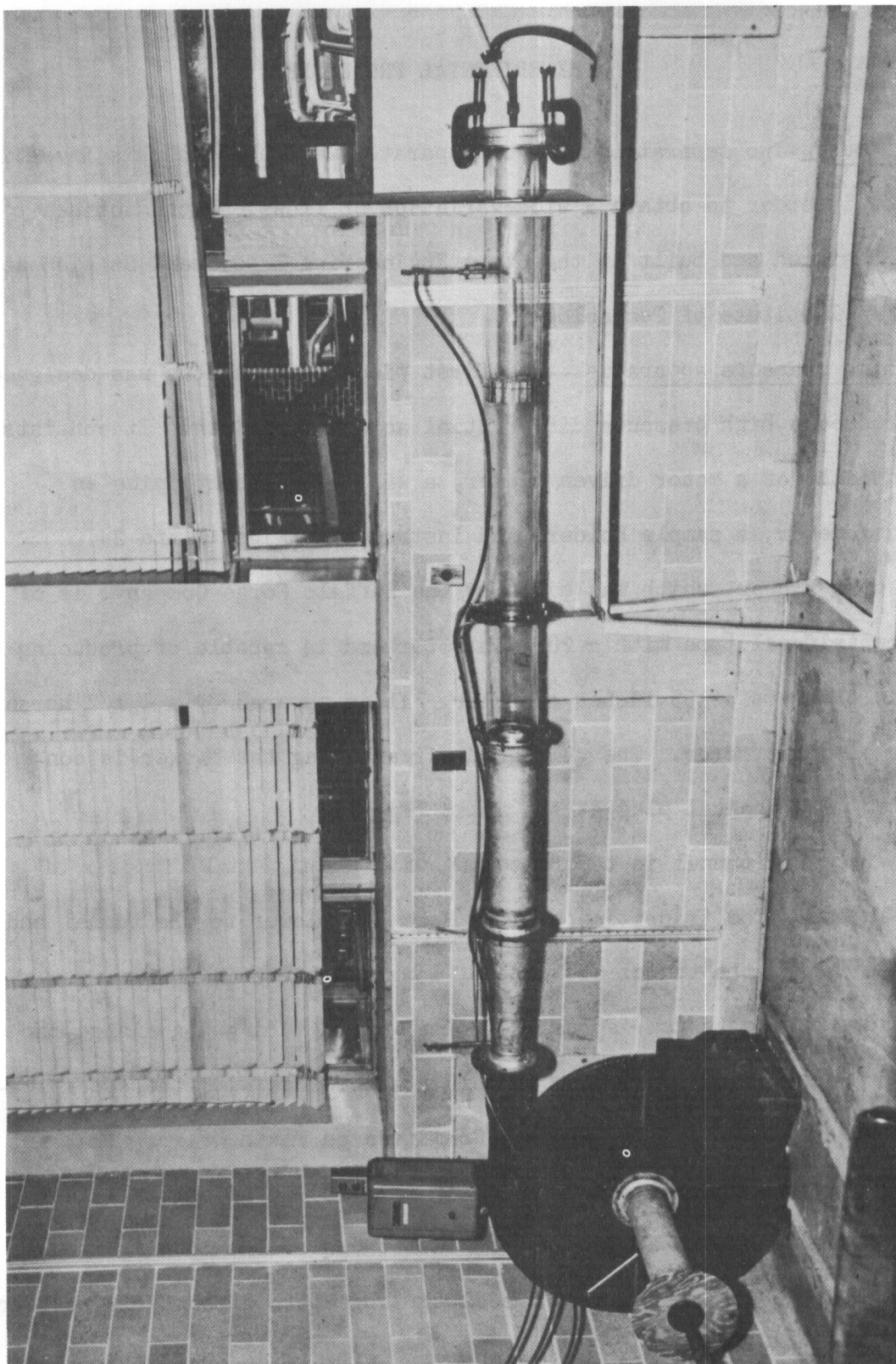


Figure 1. Test Setup.

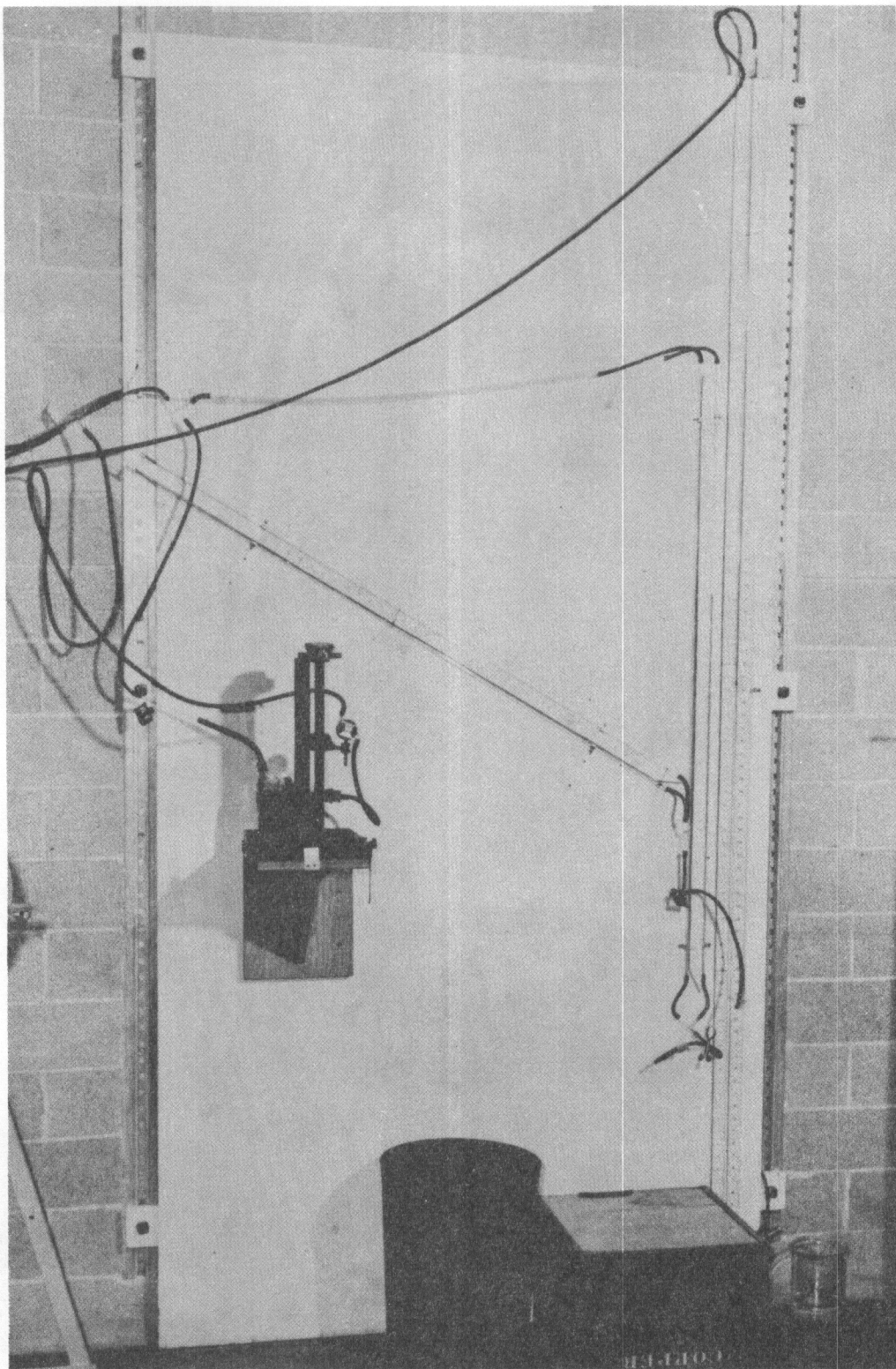


Figure 2. Gauge Board.

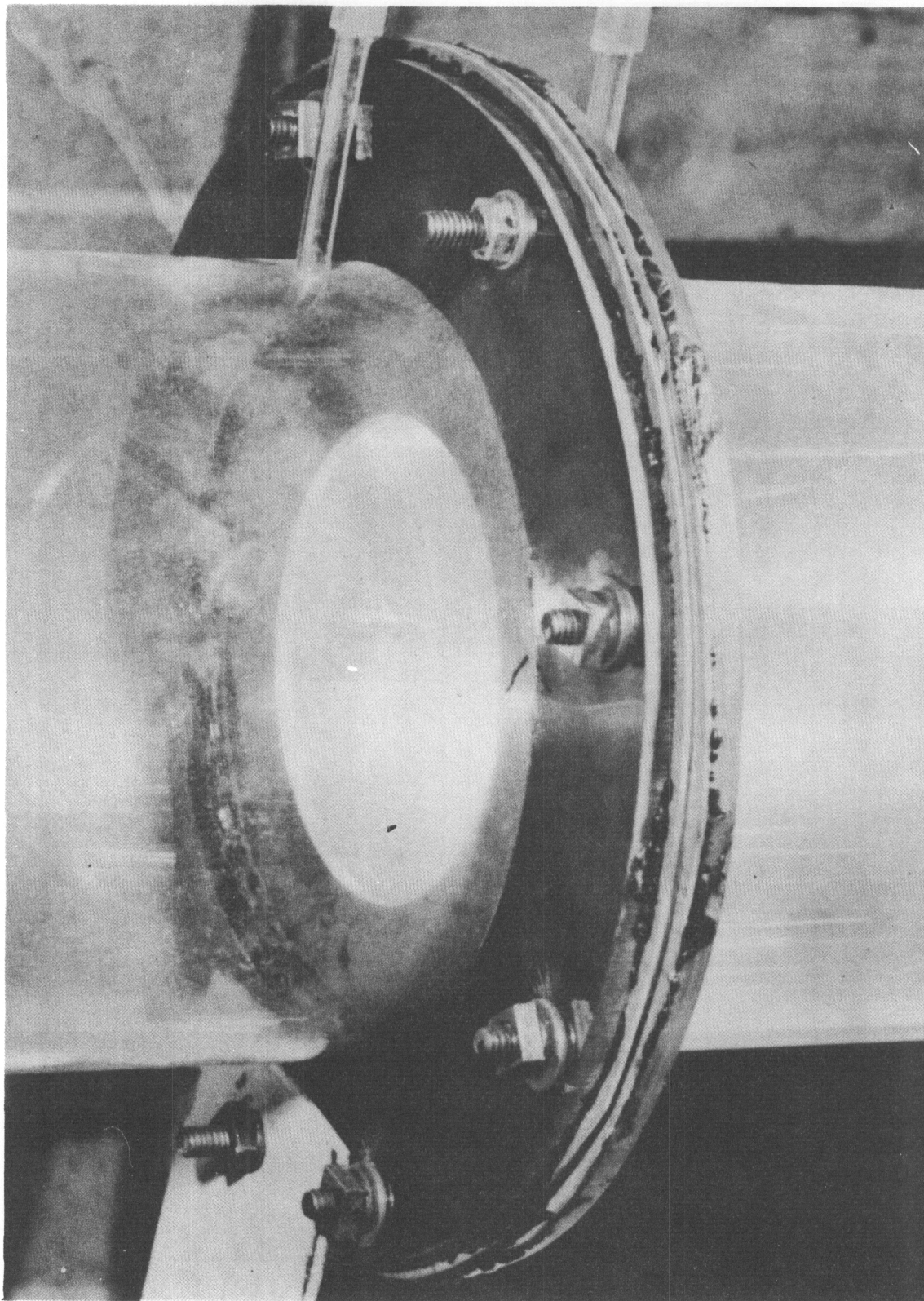


Figure 3. Typical Orifice Installation.

WADC TR 54-199

Contrails

The sample holder consists of two aluminum discs, each twelve inches in diameter (Figs. 4, 5, and 6). The upstream disc has a center hole 6.05 inches in diameter, thus, exposing to the flow an area of 0.2 square feet of cloth. The downstream disc has a center opening of 5.75 inches, the same diameter as the inside of the tunnel. The inner edge is beveled to prevent damage to the fabric. Seven screws are used to maintain pressure between the two discs, which are kept in alignment by two tapered dowell pins. Slippage between the sample and the faces of the discs is prevented by a ring made of 1/4 inch rubber tubing, which forces the edge of the sample into a concentric groove cut into the face of the upstream disc. Two similar rubber rings are used to prevent the leakage of air between the sample holder and the tunnel (Fig. 5).

The static pressure upstream of the cloth is measured by a pitot tube located 15 inches upstream of the cloth and connected to a water-filled U-tube manometer. A micromanometer using alcohol as the fluid is used to measure pressure differentials across the orifice less than eight inches of alcohol; a U-tube manometer is necessary for higher pressure differentials. Mercury thermometers are used to measure the temperature of the air at the inlet and at the outlet.

An air filter (not shown), with fiberglass filter pads in a plywood frame, encloses the intake to clean the entering air. The plywood duct built around the outlet is used to remove the heated air from the room.

The low pressure apparatus.---In order to obtain pressure differentials in the range 0-2 inches of water a second piece of apparatus was de-

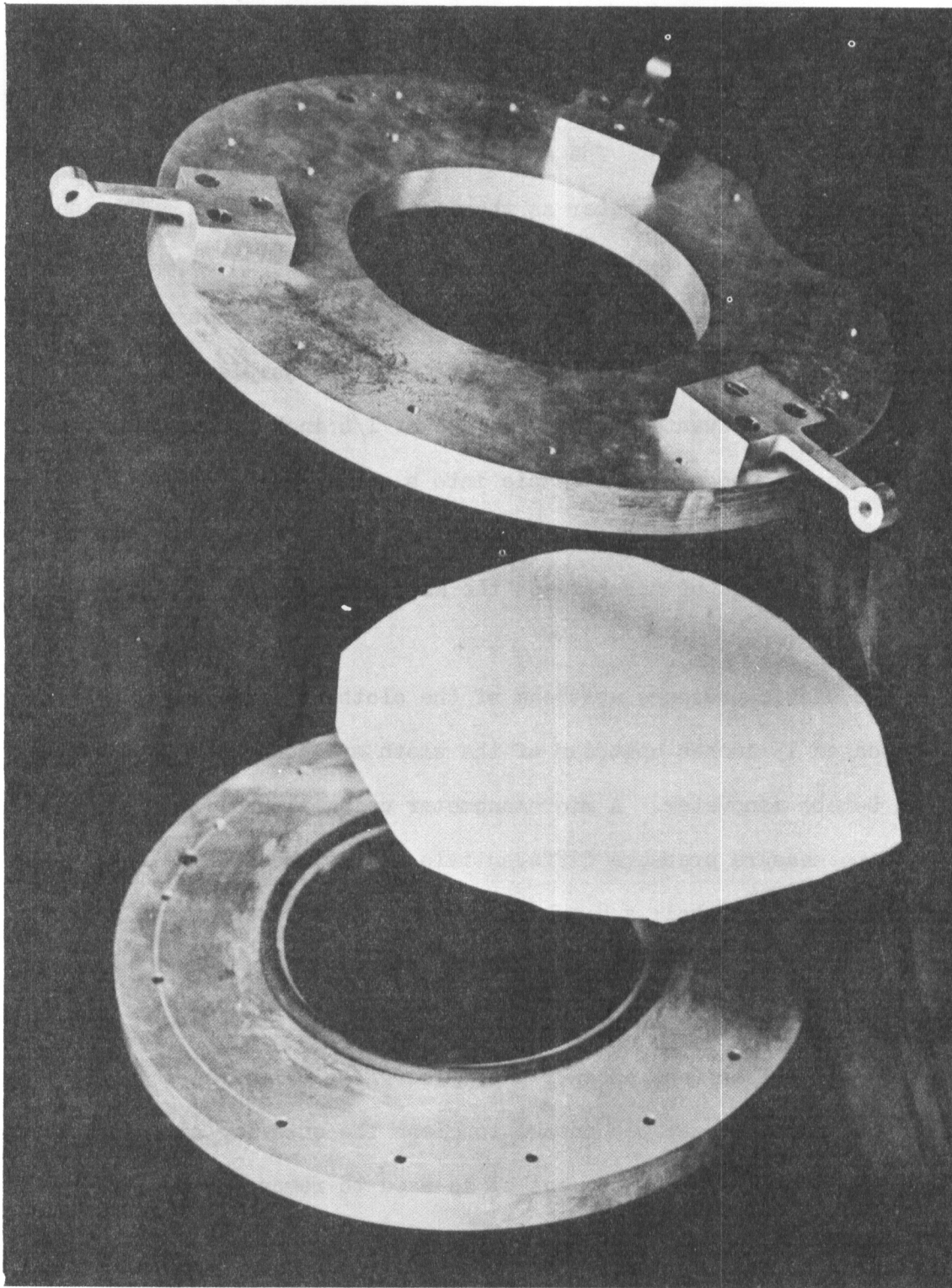


Figure 4. Exploded View of Low-Pressure Sample Holder.

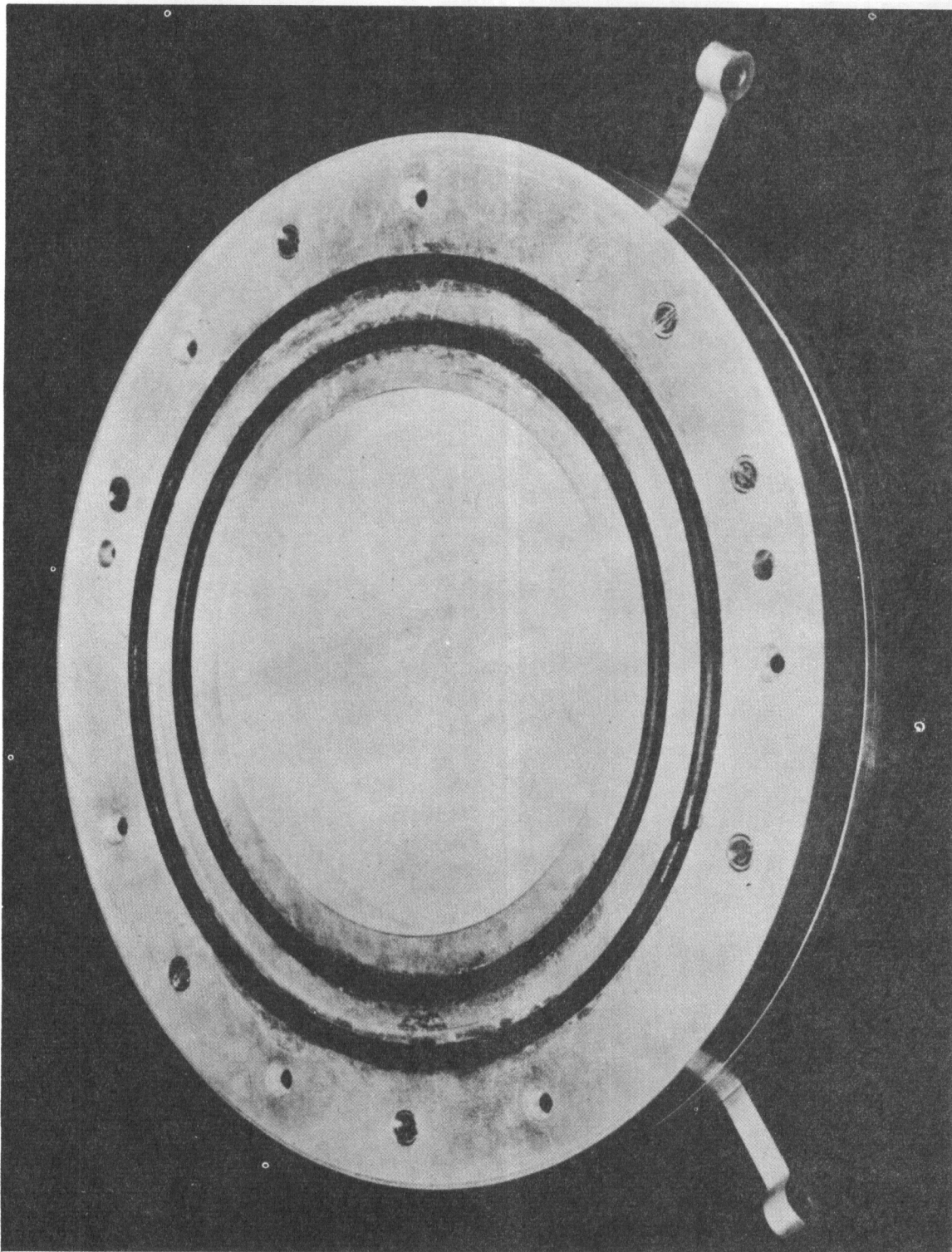


Figure 5. Upstream Face of Sample Holder.

WADC TR 54-199

17

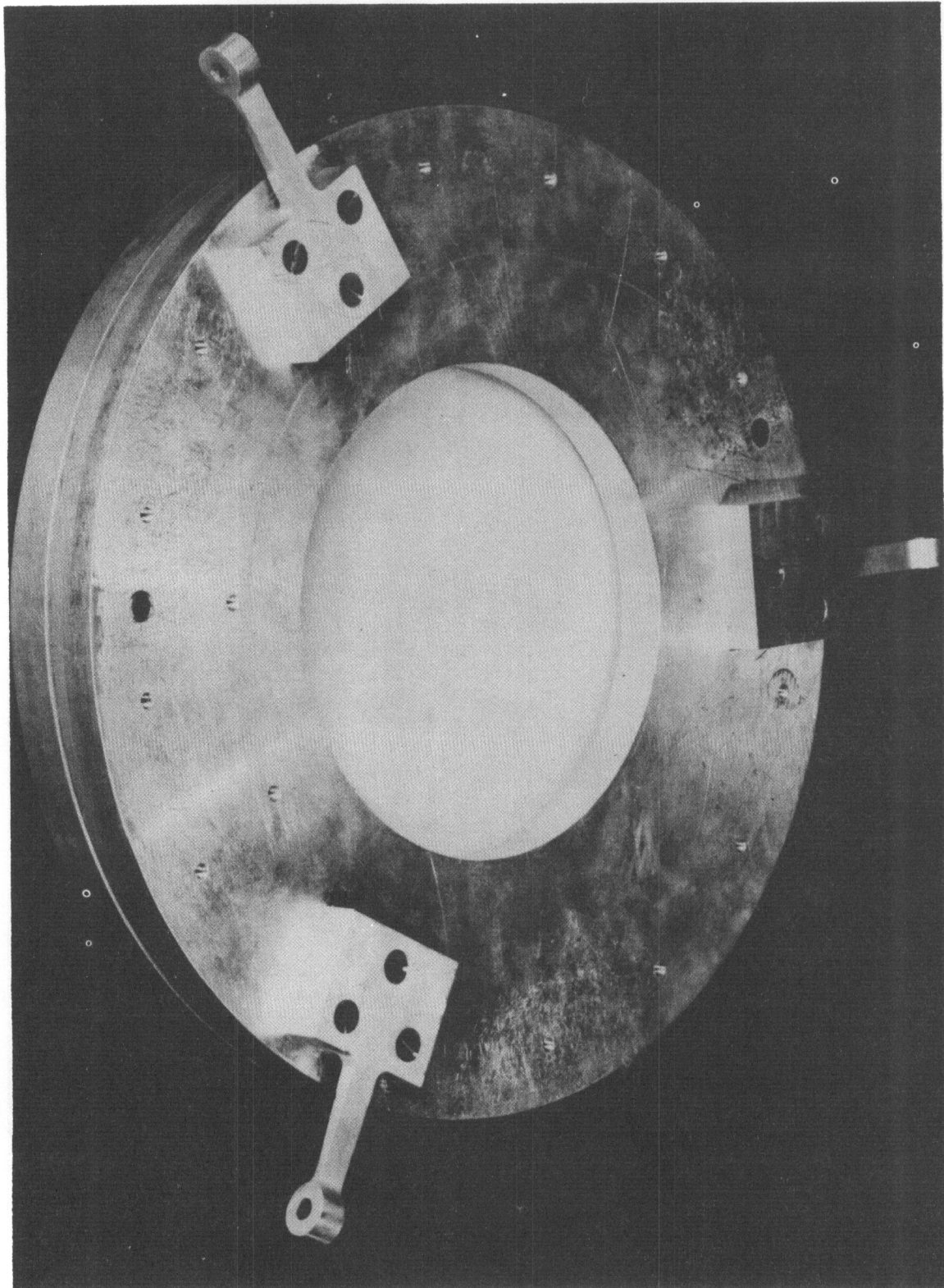


Figure 6. Downstream Face of Sample Holder.

signed, consisting of the same components as the high pressure apparatus (Fig. 7).

A vacuum cleaner motor and blower are used to furnish the air. The section of the wind tunnel containing the orifice is made of plexiglass tubing with an internal diameter of 2.75 inches. The orifice meter is again of the flange-tap type built to the specifications of the ASME Special Research Committee on Fluid Meters (12). This section of the tunnel opens into an 18 inch section of 5.75 inch plexiglass tubing with a flange arrangement on the outlet end similar to that on the high pressure tunnel. This permits the use of the same sample holder on both tunnels. The flow is controlled by a simple slide valve on the blower inlet. The static pressure and the orifice differential are measured by micromanometers using alcohol as the fluid.

Test Procedure

Sampling technique.--Since it has been shown that the permeability varies in the direction of both the warp threads and the filling threads (13), a statistical survey of the cloth was taken to determine the best method of sampling. It was found that for fabrics of the usual width (30 to 36 inches) a sample with its center 12 inches from the selvedge will provide an average representation of a section across the cloth. A further statistical study showed that the average of the permeability results of nine specimens would be within seven per cent of the true mean value 95 per cent of the time. It was decided that the slight increase in accuracy gained by taking more samples would not justify the additional cost of a larger number of tests. Since the fabrics

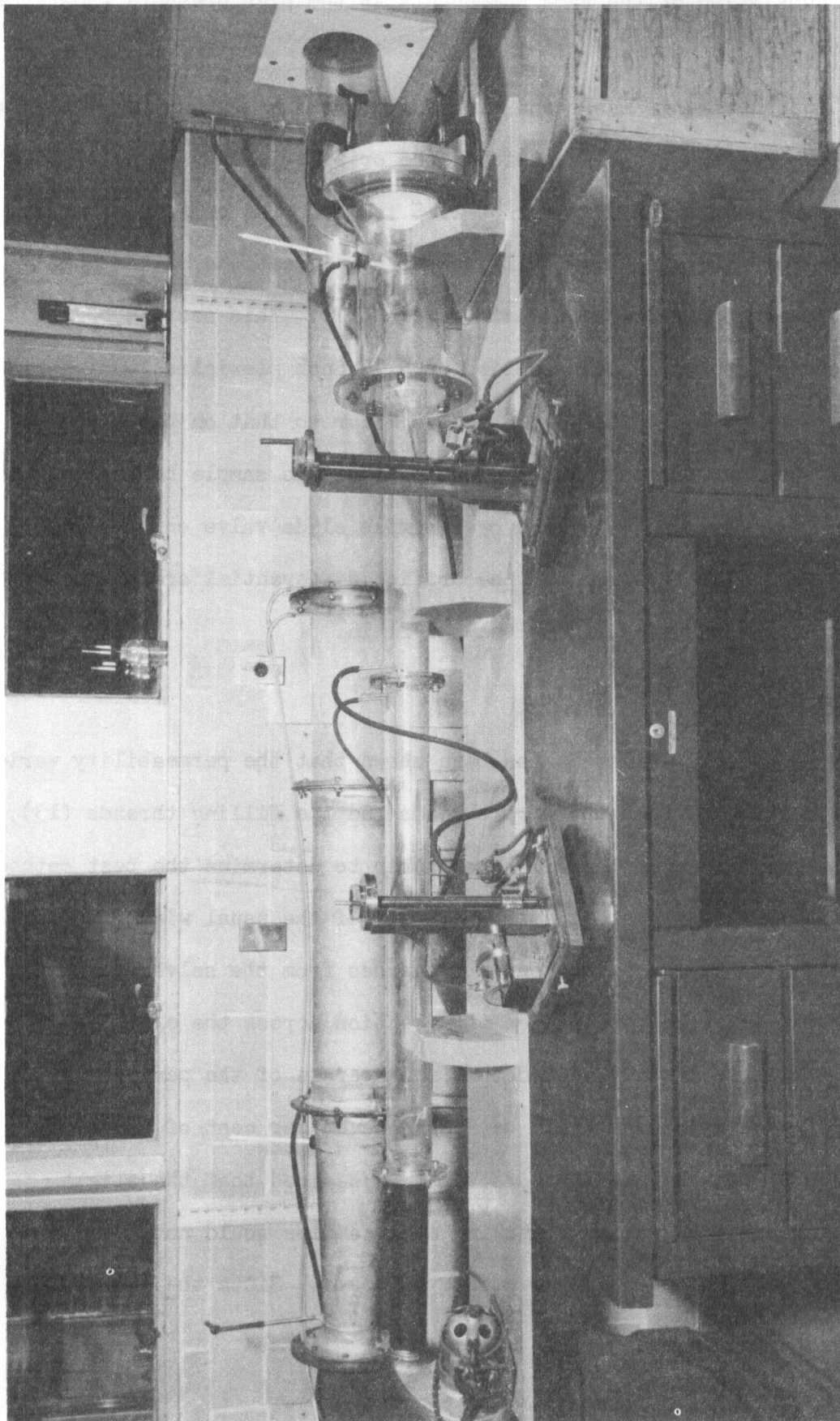


Figure 7. Low Pressure Tunnel

WADDC TR 54-199

woven by the Bally Ribbon Mills were only eight inches wide, the entire width was used for the test, but the samples were taken at intervals of five yards along the cloth.

Mounting the sample.--The front section of the sample holder is placed face down on a table and the center hole fitted with a plastic disc which is flush with the surface of the holder. The sample, which is cut circular to a diameter of eight inches, is placed on this half of the holder. Another plastic disc five inches in diameter is placed over the center of the sample to keep it smooth. The rubber ring is fitted over the groove and the second half of the holder set in place. The rubber ring is then compressed evenly by tightening the seven screws a few turns at a time in rotation. This insures that the sample is clamped evenly in the holder with a negligible amount of initial tension. The sample holder is then securely fastened to the end of the wind tunnel by three C-clamps. Repeated tests on the same sample have shown that the variations in results due to the technique of mounting the sample are negligible.

High pressure runs.--With the sample in place, the blower is started with the intake valve closed and allowed to run until the outlet temperature rises to approximately 118° F. The valve is then opened suddenly to closely simulate the shock of a suddenly opening parachute. Readings are taken of the static pressure, the orifice pressure drop, and the inlet and outlet air temperatures. Observations are made for 12 different flow conditions ranging from maximum to minimum. A barometric reading is recorded for each run.

Low Pressure runs.--The procedure for tests in the low pressure tunnel

is the same as for the high pressure tunnel with the exceptions that the steady-state operating temperature is about 83° F. and only five observations are taken for each sample.

Calculations

In order to reduce the labor involved in making the flow calculations, the data were first put through an averaging process. This process consisted of plotting a curve of the static pressure versus the orifice pressure drop for each of the nine samples, and then averaging the values of the orifice pressure drop for the nine samples at selected static pressures. An example of this averaging process, together with other sample calculations, is given in Appendix B.

TEST RESULTS

Description of samples.--The items used in this study consisted of 14 nylon fabrics and four woven wire screens.

In order to eliminate variations in permeability due to different manufacturing processes, the fabrics for test were selected from a group of ribbon cloths woven by the Bally Ribbon Mills and subjected to the same finishing processes. These fabrics were eight inches wide with selvedge at each edge. The physical properties of these fabrics, which were of varying texture and weave, are shown in Table 1.

The wire screens were standard testing screens woven by the W.S. Tyler Company. They were included in this study in order to have some fabric-like samples that are known to undergo no change in structural geometry during testing. Physical dimensions of these screens are given in Table 22.

Data and Results.--The test results for these fabrics and screens are presented in summary form in Tables 2 through 19. Typical ψ versus G curves are shown in Figs. 8 through 12. In the case of the fabrics, the values of ψ and G for these curves were obtained from averaged data and are not shown on these curves. However, the experimental points for the screens are shown, as the original test values were not averaged.

These curves show that the ψ - G relation is linear in the range of low flows, but is non-linear for higher flows. Therefore, the parameters α and β were determined from the data for the low flows

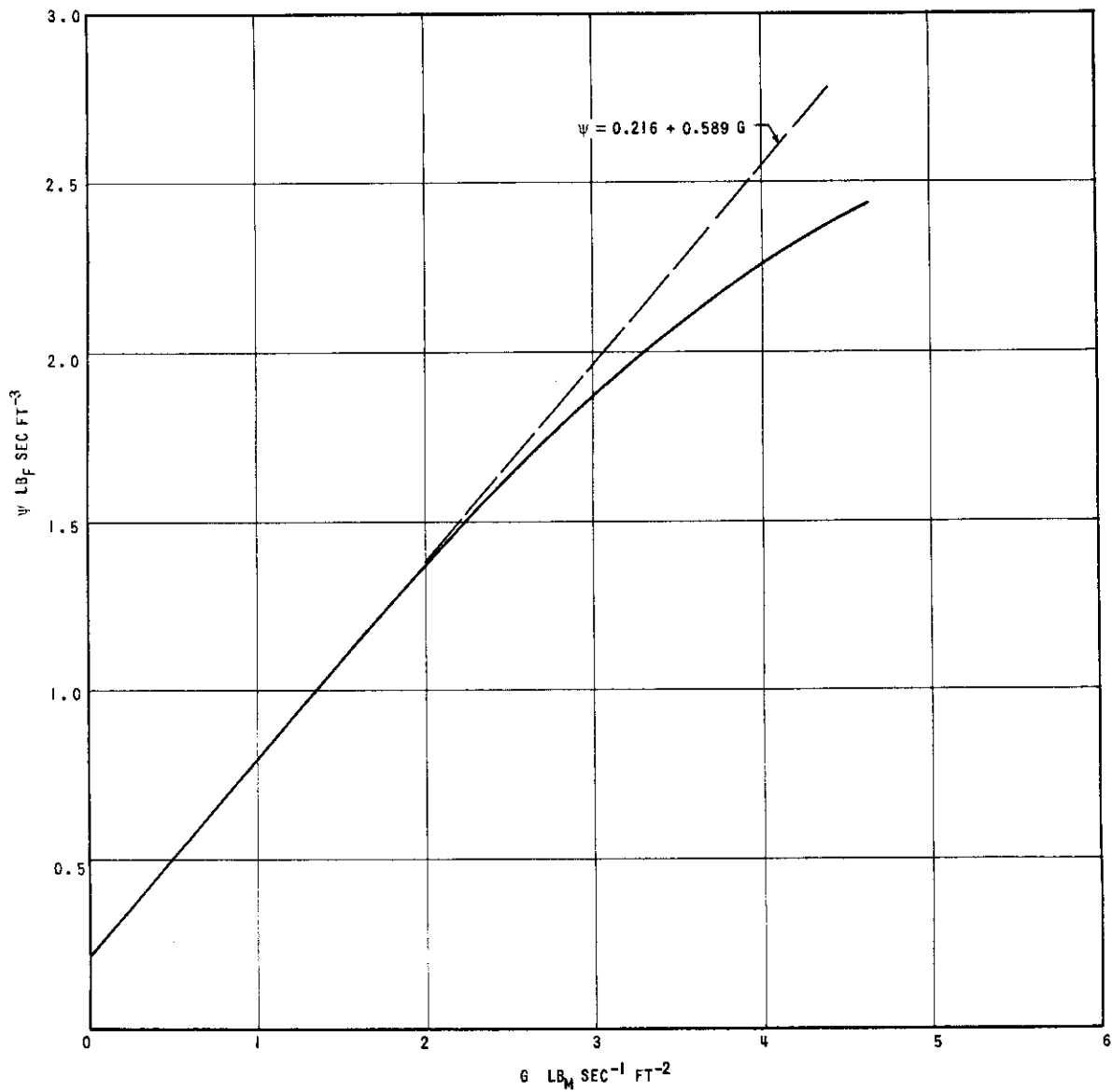


Figure 8. ψ versus Mass Velocity for Fabric BR-1

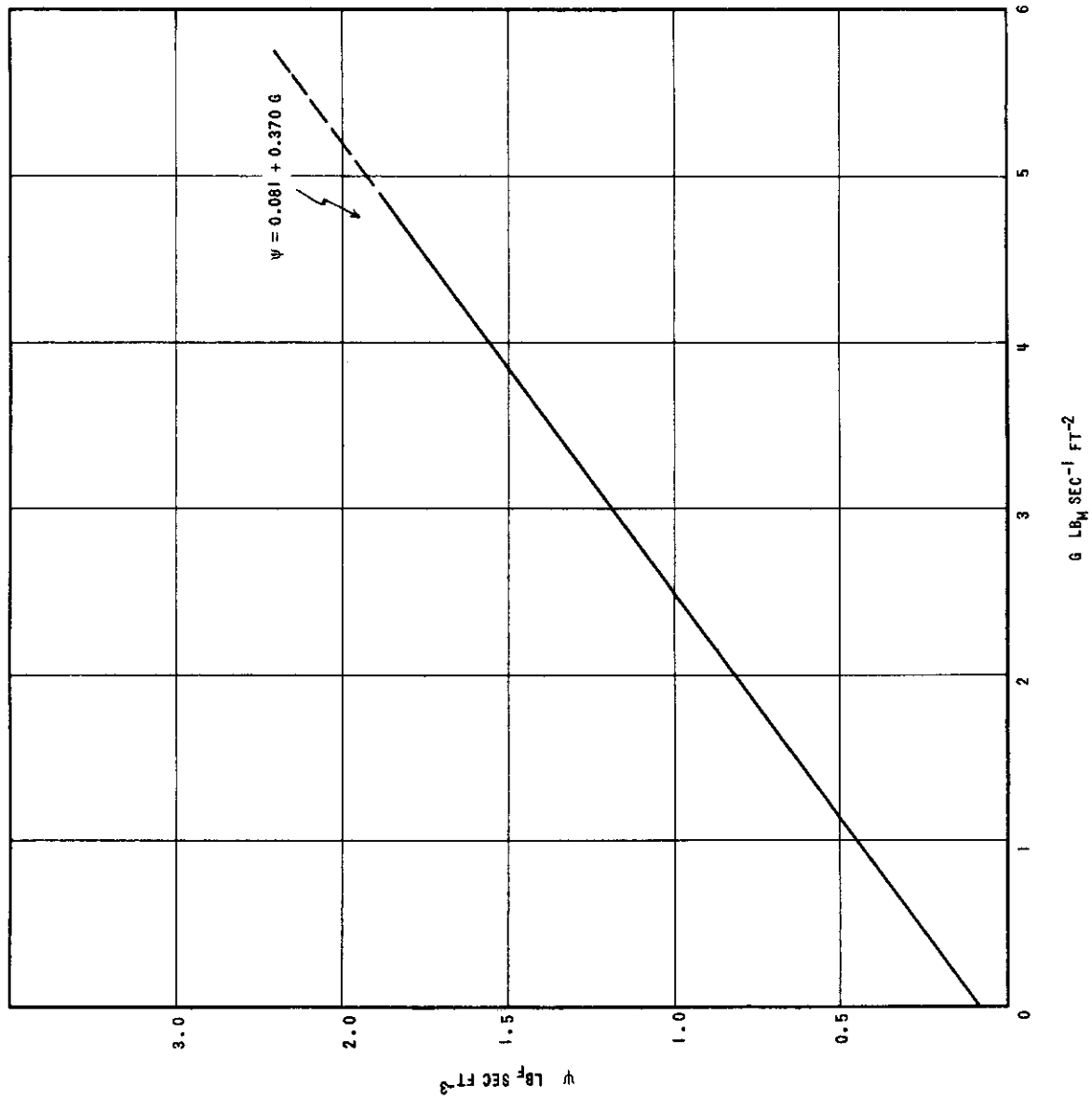


Figure 9. ψ versus Mass Velocity for Fabric BR-30

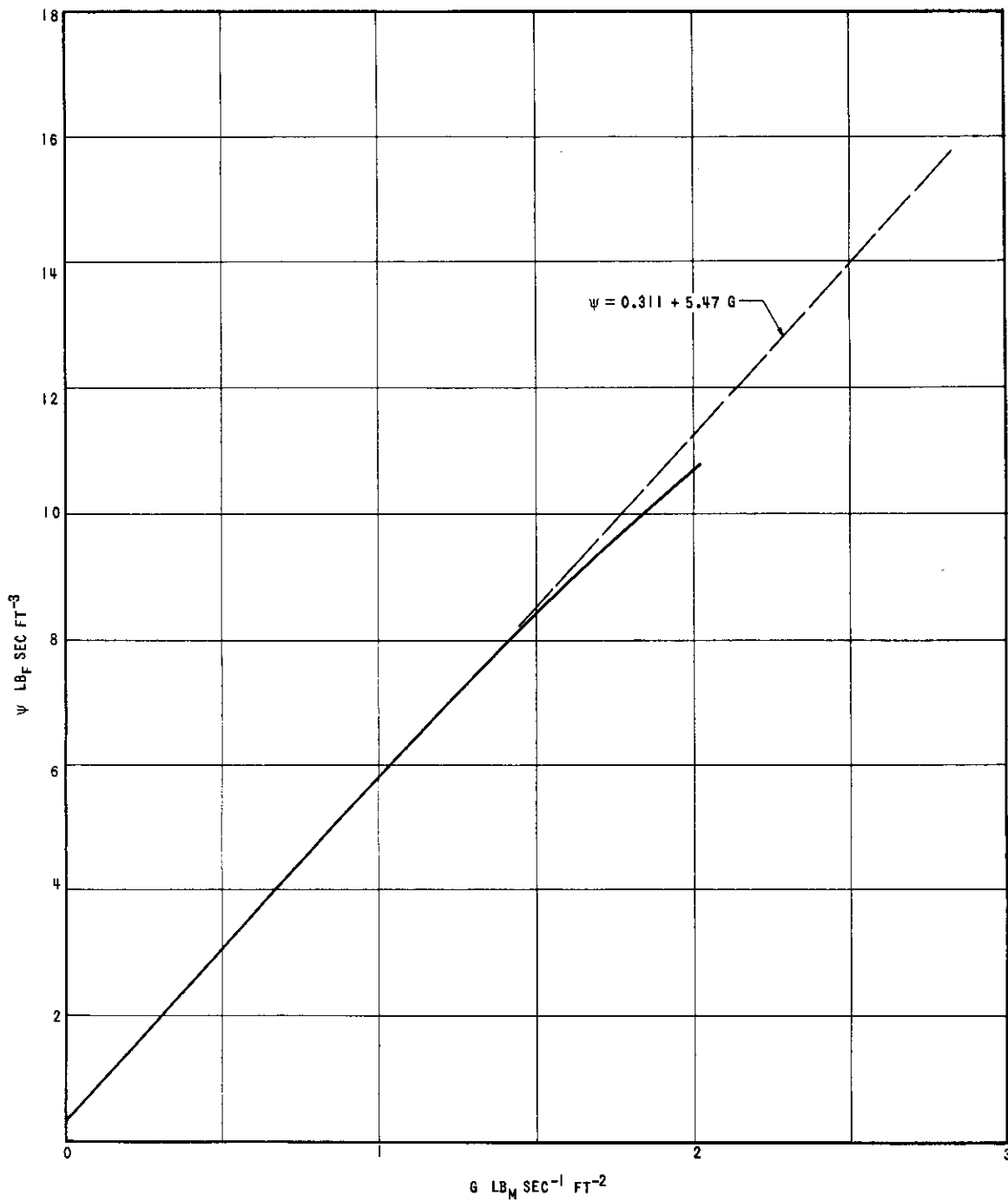


Figure 10. ψ versus Mass Velocity for Fabric BR-40

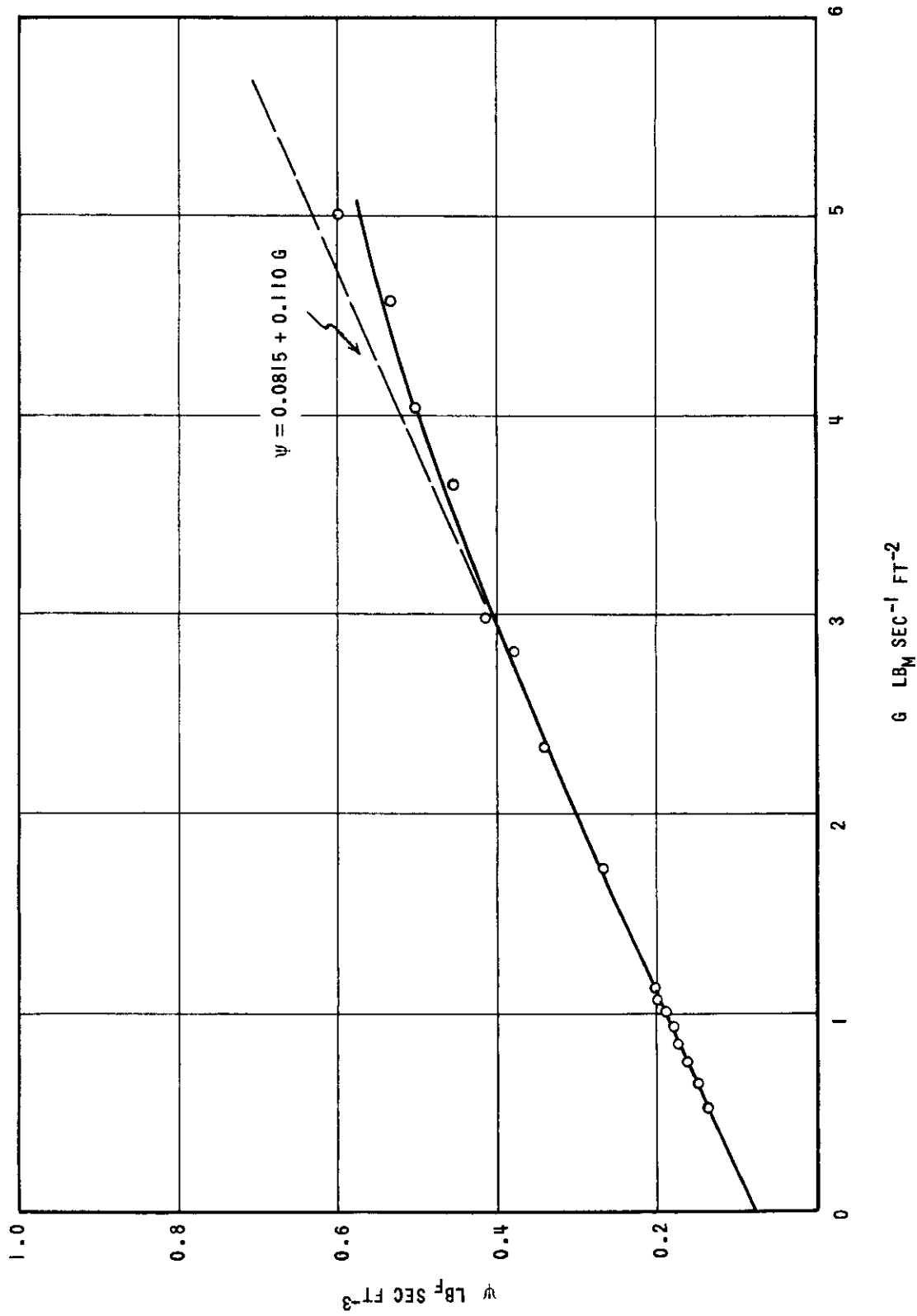


Figure 11. ψ versus Mass Velocity for 100 Mesh Screen.

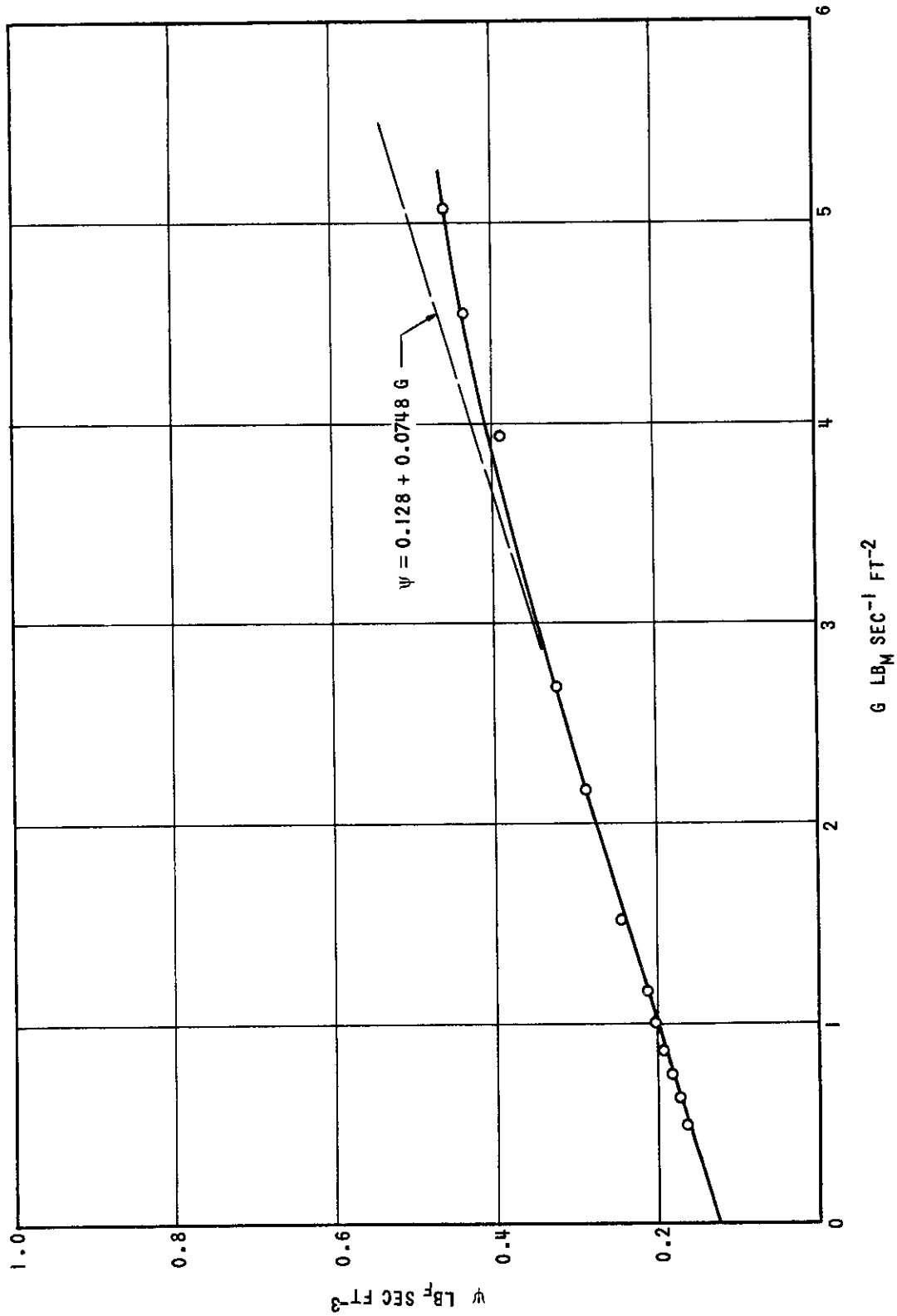


Figure 12. ψ versus Mass Velocity for 270 Mesh Screen.

only. These parameters were found by using the method of averages to fit the data to a curve of the form

$$\psi = a + bG \quad (11)$$

where

$$a = \frac{\alpha L \mu}{\epsilon_c} \quad (12)$$

and

$$b = \frac{\beta L}{\epsilon_c} \quad (13)$$

The values obtained for αL , βL , α , and β are given in Table 20.

Discussions of the results.--These results indicate that in the low range the flow is governed by the law

$$\psi = a + bG \quad (11)$$

They also indicate that for each cloth there is a rate of flow at which the permeability changes and the above law is no longer valid. From the definition of ψ in equation (9) it is seen that, for a given pressure differential, a decrease in the value of ψ implies an increase in the value of G . Hence, it implies an increase in the permeability of the fabric.

The decrease in the slope of the ψ - G curve could be a result of the deformation of the cloth, a change in the flow pattern around the threads, or a combination of both. Either of these would mean that the parameters α and β no longer characterize the flow. Since the curves for the screens exhibit this same tendency (Figs. 11 and 12), it seems

likely that most of the effect is due to a change in the flow pattern. The geometry of the pore opening is too complex for a direct comparison of the flow pattern through such an opening with the flow pattern about a cylinder, but the patterns of both exhibit some of the same trends. Goldstein (14) states that the flow past a cylinder changes from a steady to an unsteady state as the Reynolds number increases, with a large change in the drag coefficient. He further states that the value of the Reynolds number at which the unsteady regime commences is uncertain, but it is probably about 50. As the Reynolds number increases the drag coefficient falls steadily to a minimum value of 0.95 at $N_{Re} = 1800$. For the fabrics the Reynolds number based on thread width at which the ψ -G curve departs from a straight line lies between 20 and 100.

As the Reynolds numbers attained in this study were less than 400, there is no basis here for the comparison of the drag coefficients of the fabrics and the cylinder in the higher range. However, in the initial study by Goglia (15) the ∇P^2 vs G curves plotted to logarithmic scales have a slope of two in the high range of flows, which indicates that the drag coefficient is constant.

Figure 13 shows the relation between the flow-through-resistance coefficient C_f and the Reynolds number based on the characteristic length B/α .

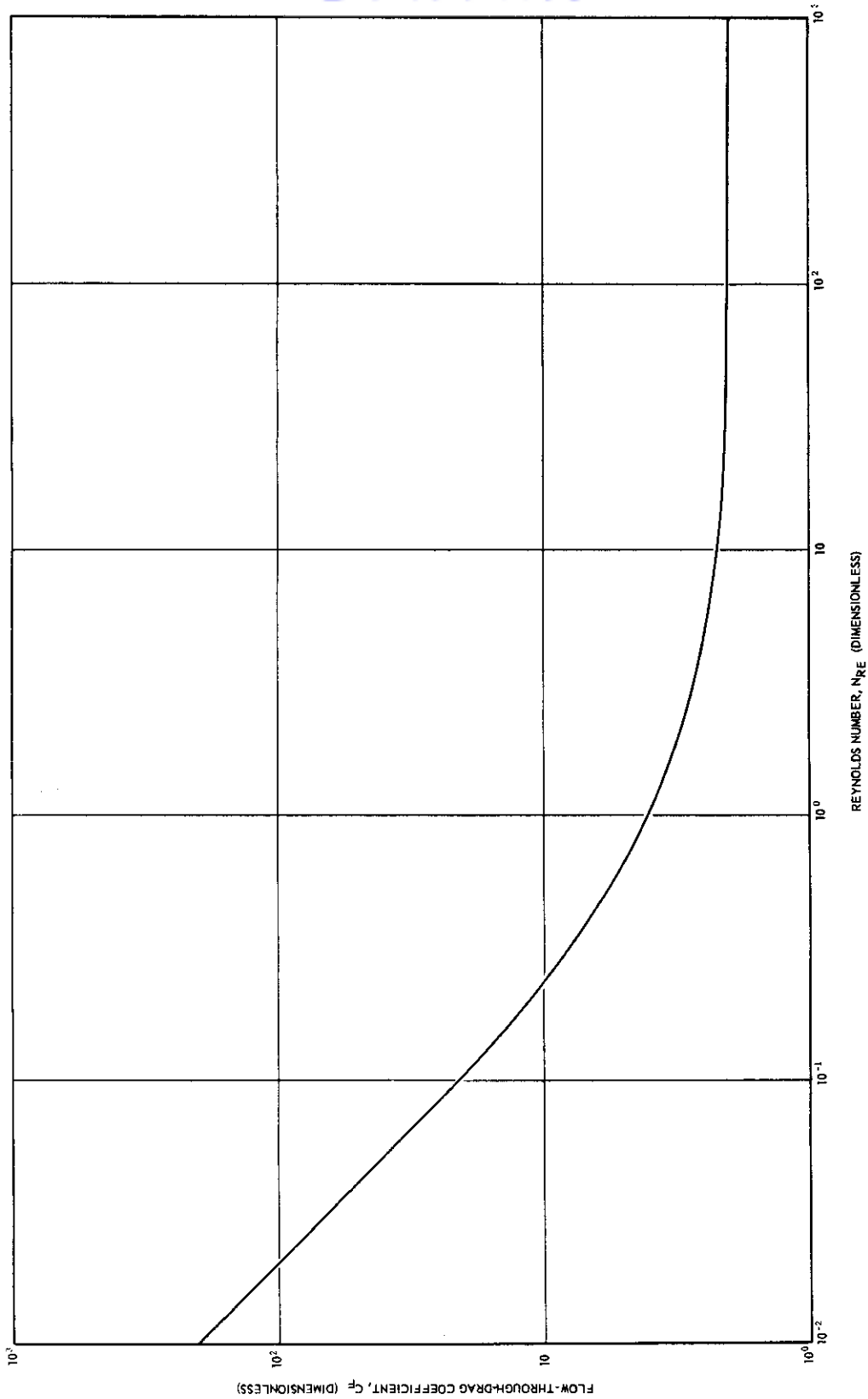


Figure 13. Relation to Flow-Through-Drag Coefficient to Reynolds Number.

PERMEABILITY PREDICTION STUDY

The value of permeability predictions.---One of the needs of the designer of textile materials for use as parachute fabrics is some means of predicting the permeability of a fabric before it is woven in order that a suitable combination of weave and texture may be selected. If the parameters α and β could be approximated from the thread dimensions and weave, a reduction could be made in the number of experimental fabrics that would have to be woven in order to obtain the desired combination of strength and permeability.

Description of samples.---The samples used in this study are the twelve plain weave ribbon cloths and the four wire screens. The selection was limited to plain weave specimens since the limited time available for this study precludes any attempt to apply Backer's theory of a minimum pore area to obtain correlation between the different types of weaves.

Measurement of thread widths.---The thread widths were obtained by measuring the width of ten adjacent threads with a filar microscope. Although the individual threads varied by as much as 100 per cent, the average width of ten adjacent threads seldom varied by more than 15 per cent. The mean value of the thread width for a particular denier was assumed to be the average after such measurements were taken from a number of samples of that denier. All threads of the same denier and twist were assumed to have the same dimensions regardless of the thread spacing. These dimensions together with the thread spacings and fabric

Contrails

thicknesses are shown in Table 21. The physical dimensions of the wire screens as given by the manufacturer are shown in Table 22.

Relation between the fabric geometry and α and β .---In the deriva-

tion of the general flow equation (5) the geometric constants which characterize the flow were included in the constants α and β .

These geometric constants include a length d_e (which is a measure of the effective diameter of the pore opening) the plane porosity ϵ , the fabric thickness L , and the surface roughness of the fibers e/d .

Since the fabrics used in this study were all nylon, it will be assumed that the value of e/d is the same for all. Under these assumptions α and β are functions of the effective diameter d_e , the plane porosity ϵ , and the thickness L .

The relations among these variables which have some semblance of continuity for both fabrics and screens are of the forms

$$\alpha L = F_1 (d_e \epsilon) \quad (12)$$

and

$$\beta L = F_2 (\epsilon) \quad (13)$$

where F_1 and F_2 are arbitrary functions of the indicated variables.

An approximate negative slope of one in Figure 14 indicates that the function F_1 is equal to the reciprocal of its argument, i.e., αL is inversely proportional to $d_e \epsilon$.

The functional relation between βL and ϵ is not clearly defined in Figure 15. For Reynolds numbers above 1000 Hoerner (16) finds the relation between the drag coefficient C_d and the solidity G of round wire screens to be

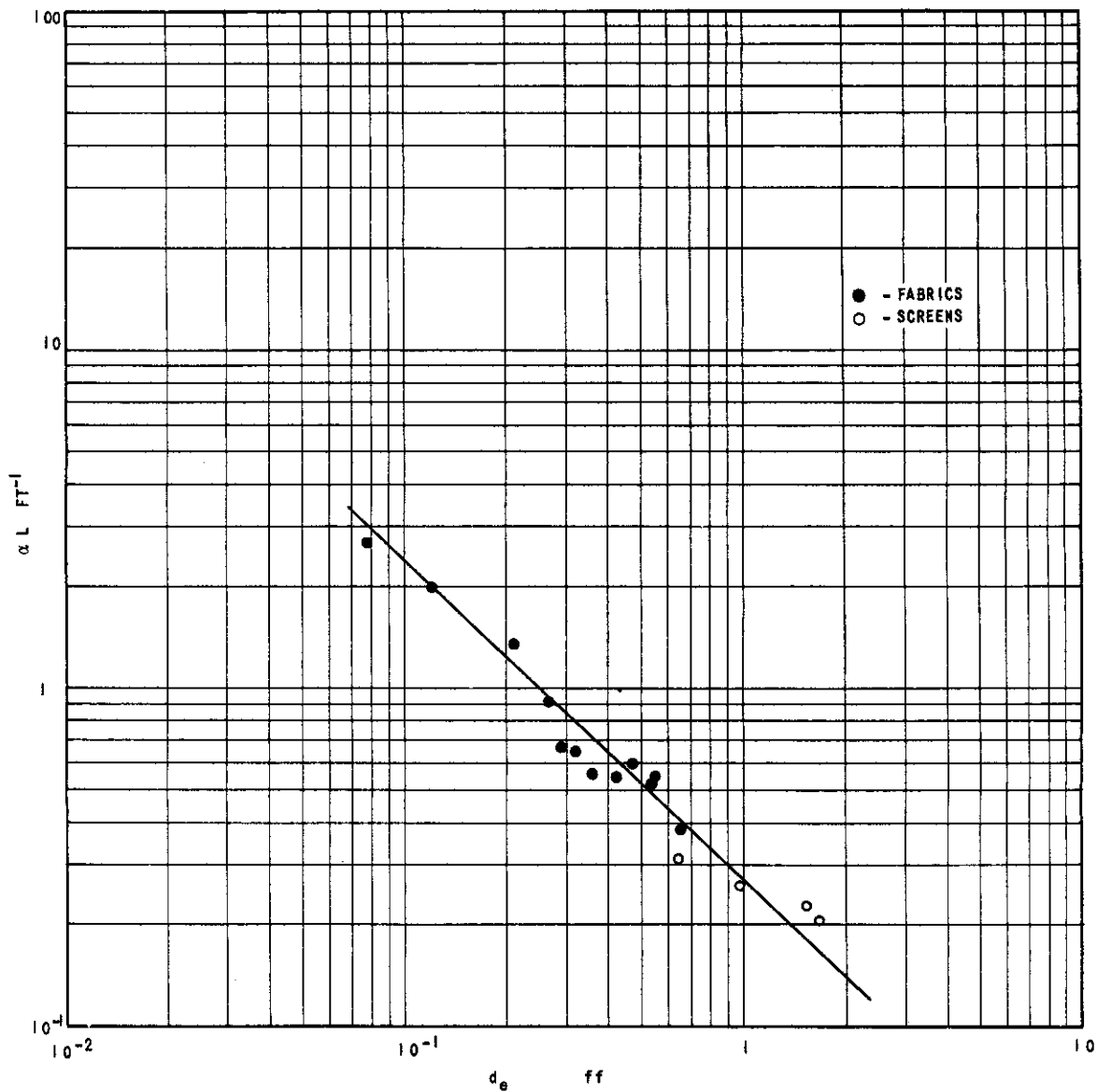


Figure 14. Relation of α to Fabric Geometry.

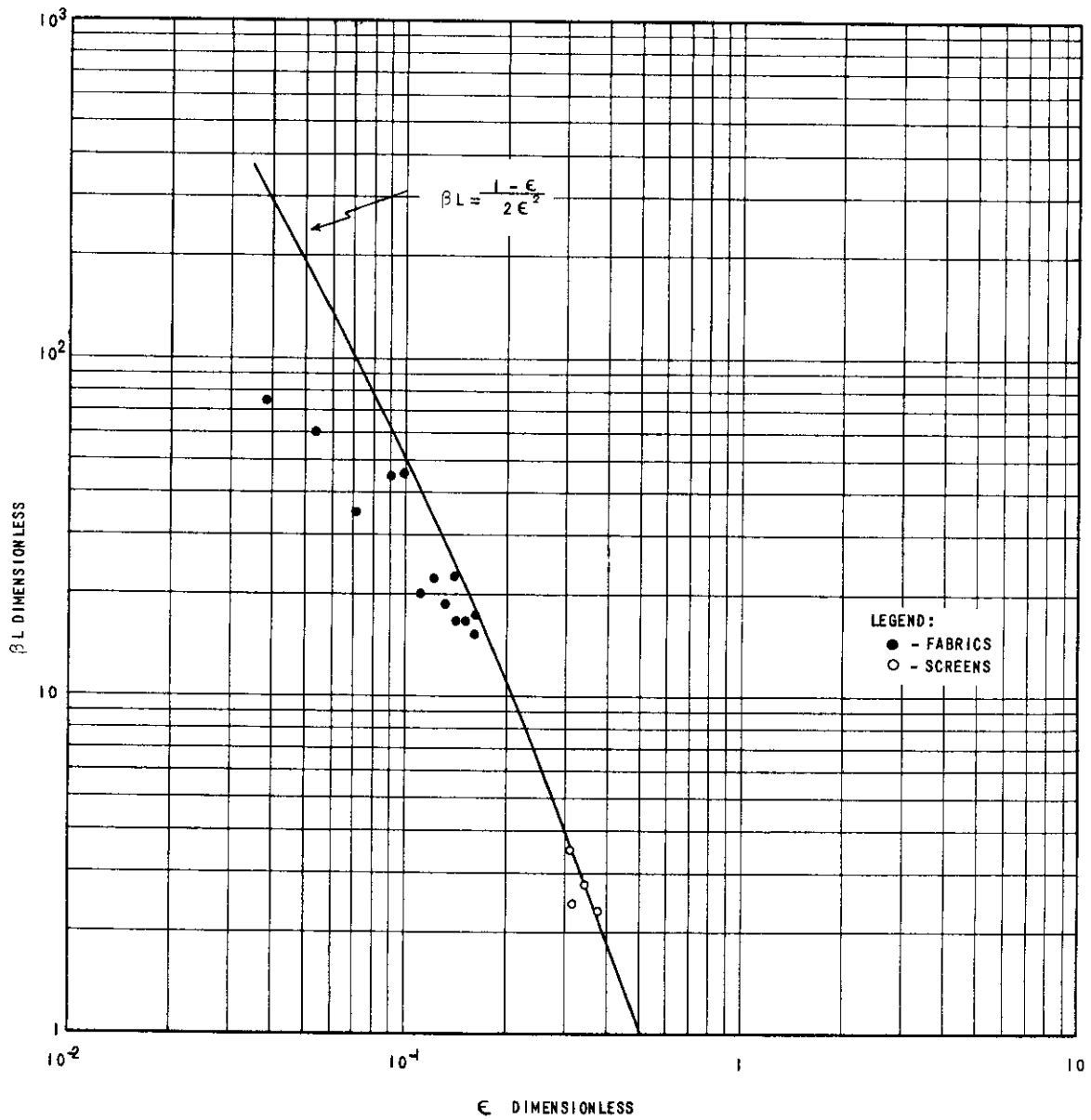


Figure 15. Relation of β to Fabric Geometry.

Contrails

$$C_d = \frac{Q}{(1 - \phi)^2} \quad (14)$$

where $Q = 1 - \epsilon$. If this relation holds in the present case the $\beta_L - \epsilon$ relation is

$$\beta_L = 1/2 \left(\frac{1 - \epsilon}{\epsilon^2} \right) \quad (15)$$

This equation, which is shown as a solid line in Figure 15, fits the data fairly well for the screens and open weave fabrics, but it does not agree with the data for the less porous fabrics. If this relation holds for both the low range and the high range of flow, it implies that the slope of the $\psi - G$ curve assumes its original value in the high range.

In the less porous fabrics the error in the measurement of the thread widths is greatly magnified in the calculated values of ϵ and d_e . Furthermore, as the number of threads per inch is increased, the point is reached at which there is no visible projected open area, but small openings are visible when the fabric is viewed from an acute angle. For these reasons it may be necessary to limit permeability predictions to the more open weave fabrics.

The β_L values of more fabrics of both low and high porosity are needed in order to justify any curve drawn through the points in Figure 15.

CHAPTER VI

CONCLUSIONS

The following conclusions may be drawn from this study:

1. Over the lower range the flow of a fluid through fabrics can be characterized by the dimensionless relation

$$C_f = \frac{2}{N_{Re}} + 2 \quad (8)$$

2. The upper limit of the range for which this equation is valid cannot be fully determined from the data available in this study.

3. The relation loses its validity because α and β become variable functions of the velocity of flow.

4. The ψ -G relation permits the determination of the parameters α and β from only two flow measurements.

5. This dimensionless relation permits the comparison of tests made on fabrics under different conditions of temperature, density, and viscosity.

6. A rough estimate of the values of α and β may be obtained from physical measurements of the cloth.

Contrails

SUMMARY OF RESULTS

TABLE 1

Physical Properties of Bally Ribbon Cloths

<u>Item Number</u>	<u>Thread Count Per Inch</u>		<u>Yarn Denier</u>		<u>Weave</u>
	<u>Warp</u>	<u>Filling</u>	<u>Warp</u>	<u>Filling</u>	
BR-1	135	113	30/10	30/10	Plain
BR-2	133	122	"	"	"
BR-5	134	99	"	40/13	"
BR-6	137	110	"	"	"
BR-9	119	85	40/13	40/34	"
BR-10	118	83	"	"	"
BR-11	122	95	"	40/13	"
BR-12	123	105	"	"	"
BR-13	123	75	"	60/20	"
BR-14	125	87	"	"	"
BR-17	100	75	60/20	"	"
BR-18	102	84	"	"	"
BR-30	92	80	70/34	70/34	5 H. Satin
BR-40	79	69	100/34	100/34	2/2 Twill

Contrails

TABLE 2

Experimental Data for Fabric Number BR-1

∇P (inches water)	ρ ($lb_m - ft^{-3}$)	G ($lb_m - sec^{-1} - ft^{-2}$)	ψ ($lb_f - sec.-ft^{-3}$)
------------------------------	--------------------------------	--	-------------------------------------

High Pressure Apparatus:

30	0.0740	4.50	2.42
25	0.0714	3.98	2.27
20	0.0705	3.47	2.07
15	0.0695	3.00	1.78
10	0.0688	2.28	1.55
8	0.0683	2.00	1.41
6	0.0681	1.71	1.24
4	0.0677	1.36	1.04
3	0.0676	1.17	0.902
2	0.0674	0.937	0.750
1	0.0672	0.636	0.552

Low Pressure Apparatus:

0.56	0.0720	0.435	0.478
0.40	0.0720	0.338	0.443
0.32	0.0720	0.292	0.407
0.24	0.0720	0.238	0.375
0.16	0.0720	0.184	0.324

Experimental Data for Fabric Number BR-2

∇P (inches water)	ρ ($lb_m - ft^{-3}$)	G ($lb_m - sec^{-1} - ft^{-2}$)	ψ ($lb_f - sec. ft^{-3}$)
High Pressure Apparatus:			
30	0.0722	4.25	2.57
25	0.0713	3.77	2.40
20	0.0705	3.28	2.19
15	0.0696	2.73	1.96
10	0.0687	2.10	1.69
8	0.0684	1.89	1.50
6	0.0678	1.61	1.31
4	0.0677	1.30	1.08
3	0.0676	1.12	0.942
2	0.0673	0.912	0.771
1	0.0672	0.637	0.552
0.56	0.0715	0.403	0.522
0.40	0.0715	0.320	0.470
0.32	0.0715	0.273	0.441
0.24	0.0715	0.227	0.398
0.16	0.0715	0.173	0.348

TABLE 4

Experimental Data for Fabric Number BR-5

∇P (inches water)	ρ ($lb_m - ft^{-3}$)	G ($lb_m - sec^{-1} - ft^{-2}$)	ψ ($lb_f - sec.ft.^{-3}$)
High Pressure Apparatus:			
30	0.0721	4.58	2.38
25	0.0712	4.12	2.19
20	0.0703	3.62	1.98
15	0.0697	3.07	1.74
10	0.0687	2.41	1.47
8	0.0678	2.14	1.32
6	0.0682	1.82	1.16
4	0.0677	1.44	0.981
3	0.0677	1.22	0.867
2	0.0663	0.995	0.705
1	0.0673	0.697	0.504
Low Pressure Apparatus:			
0.48	0.0715	0.422	0.430
0.40	0.0715	0.373	0.403
0.32	0.0715	0.320	0.376
0.24	0.0715	0.259	0.348
0.16	0.0715	0.196	0.307

Experimental Data for Fabric Number BR-6

∇P (inches water)	ρ ($lb_m - ft^{-3}$)	G ($lb_m - sec^{-1} - ft^{-2}$)	ψ ($lb_f sec. ft.^{-3}$)
High Pressure Apparatus:			
30	0.0716	3.95	2.76
25	0.0707	3.54	2.55
20	0.0698	3.11	2.31
15	0.0690	2.21	*
10	0.0682	2.08	1.70
8	0.0678	1.84	1.54
6	0.0675	1.56	1.36
4	0.0672	1.26	1.12
3	0.0670	1.09	0.968
2	0.0668	0.889	0.788
1	0.0667	0.616	0.569

Low Pressure Apparatus:

0.56	0.0715	0.399	0.526
0.40	0.0715	0.316	0.475
0.32	0.0715	0.268	0.449
0.24	0.0715	0.221	0.408
0.16	0.0715	0.167	0.360

* Data not available.

Experimental Data for Fabric Number BR-9

∇P (inches water)	ρ (lb _m - ft ⁻³)	G (lb _m - sec ⁻¹ - ft ⁻²)	ψ (lb _f sec. ft ⁻³)
High Pressure Apparatus:			
30	0.0718	4.37	2.50
25	0.0710	3.93	2.30
20	0.0700	3.46	2.08
15	0.0693	2.96	1.80
10	0.0686	2.36	1.50
8	0.0683	2.09	1.35
6	0.0678	1.79	1.18
4	0.0675	1.45	0.973
3	0.0671	1.25	0.845
2	0.0659	1.00	0.701
1	0.0650	0.695	0.504

Low Pressure Apparatus:

0.48	0.0710	0.419	0.431
0.40	0.0710	0.367	0.410
0.32	0.0710	0.322	0.374
0.24	0.710	0.256	0.352
0.16	0.0710	0.196	0.307

TABLE 7

Experimental Data for Fabric Number BR-10

∇P (inches water)	ρ ($lb_m - ft^{-3}$)	G ($lb_m - sec^{-1} - ft^{-2}$)	ψ ($lb_f sec.ft.^{-3}$)
High Pressure Apparatus:			
30	0.0719	4.85	2.25
25	0.0710	4.26	2.12
20	0.0702	3.72	1.93
15	0.0694	3.18	1.68
10	0.0685	2.58	1.38
8	0.0682	2.27	1.25
6	0.0678	1.94	1.09
4	0.0675	1.57	0.898
3	0.0673	1.35	0.780
2	0.0672	1.09	0.644
1	0.0669	0.756	0.464
Low Pressure Apparatus:			
0.40	0.0710	0.435	0.345
0.32	0.0710	0.373	0.322
0.24	0.0710	0.307	0.294
0.16	0.0710	0.232	0.259
0.08	0.0710	0.140	0.215

Contrails

TABLE 8

Experimental Data for Fabric Number BR-11

∇P (inches water)	ρ ($lb_m - ft^{-3}$)	G ($lb_m - sec^{-1} - ft^{-2}$)	ψ ($lb_f sec. ft^{-3}$)
High Pressure Apparatus:			
30	0.0720	4.41	2.47
25	0.0711	3.94	2.29
20	0.0703	3.49	2.06
15	0.0694	2.92	1.83
10	0.0681	2.34	1.52
8	0.0682	2.08	1.36
6	0.0679	1.78	1.19
4	0.0676	1.43	0.986
3	0.0674	1.22	0.867
2	0.0672	0.983	0.714
1	0.0671	0.660	0.530

Low Pressure Apparatus:

0.48	0.0710	0.414	0.436
0.40	0.0710	0.365	0.412
0.32	0.0710	0.312	0.386
0.24	0.0710	0.259	0.348
0.16	0.0710	0.199	0.302

Contrails

TABLE 9

Experimental Data for Fabric Number BR-12

∇P (inches water)	ρ ($lb_m - ft^{-3}$)	G ($lb_m - sec^{-1} - ft^{-2}$)	ψ ($lb_f - sec.ft.^{-3}$)
High Pressure Apparatus:			
40	0.0733	4.58	3.21
30	0.0718	3.80	2.87
25	0.0708	3.41	2.65
20	0.0700	2.98	2.41
15	0.0692	2.54	2.10
10	0.0684	2.01	1.76
8	0.0680	1.78	1.59
6	0.0677	1.52	1.39
4	0.0674	1.23	1.15
3	0.0673	1.07	0.986
2	0.0671	0.850	0.823
1	0.0668	0.587	0.596

Low Pressure Apparatus:

0.56	0.0710	0.398	0.526
0.40	0.0710	0.313	0.479
0.32	0.0710	0.269	0.447
0.24	0.0710	0.224	0.403
0.16	0.0710	0.173	0.348

Contrails

TABLE 10

Experimental Data for Fabric Number BR-13

∇P (inches water)	ρ ($lb_m - ft^{-3}$)	G ($lb_m - sec^{-1} - ft^{-2}$)	ψ ($lb_f sec. ft.^{-3}$)
High Pressure Apparatus:			
40	0.0736	3.17	4.64
30	0.0720	2.67	4.08
25	0.0711	2.39	3.78
20	0.0703	2.11	3.40
15	0.0694	1.79	3.23
10	0.0686	1.43	2.48
8	0.0682	1.27	2.23
6	0.0679	1.10	1.93
4	0.0676	0.893	1.58
3	0.0674	0.770	1.37
2	0.0672	0.621	1.13
1	0.0671	0.434	0.806

Low Pressure Apparatus:

0.96	0.0712	0.379	0.954
0.64	0.0712	0.296	0.813
0.48	0.0712	0.248	0.728
0.32	0.0712	0.204	0.592
0.16	0.0712	0.138	0.436

Contrails
TABLE XI

Experimental Data for Fabric Number BR-14

∇P (inches water)	ρ ($lb_m - ft^{-3}$)	G ($lb_m - sec^{-1} - ft^{-2}$)	ψ ($lb_f sec. ft^{-3}$)
High Pressure Apparatus:			
50	0.0755	2.79	6.66
45	0.0746	2.57	6.48
40	0.0738	2.41	6.09
30	0.0721	2.03	5.39
20	0.0704	1.60	4.47
10	0.0687	1.09	3.25
7	0.0682	0.907	2.73
4	0.0677	0.680	2.08
3	0.0675	0.591	1.79
2	0.0674	0.489	1.43
1	0.0672	0.383	0.915

Low Pressure Apparatus:

1.44	0.0712	0.362	1.49
1.12	0.0712	0.300	1.40
0.80	0.0712	0.243	1.24
0.48	0.0712	0.170	1.06
0.16	0.0712	0.082	0.733

Experimental Data for Fabric Number Br-17

∇P (inches water)	ρ ($lb_m - ft^{-3}$)	G ($lb_m - sec^{-1} - ft^{-2}$)	ψ ($lb_f Sec. ft^{-3}$)
------------------------------	--------------------------------	--	-----------------------------------

High Pressure Apparatus:

50	0.0751	3.70	5.04
45	0.0743	3.47	4.82
40	0.0734	3.23	4.56
30	0.0717	2.73	3.99
20	0.0701	2.18	3.29
10	0.0684	1.48	2.40
4	0.0674	0.933	1.51
3	0.0672	0.805	1.31
2	0.0671	0.664	1.06
1	0.0669	0.467	0.749

Low Pressure Apparatus:

1.12	0.0712	0.405	1.04
0.88	0.0712	0.344	0.964
0.64	0.0712	0.278	0.865
0.40	0.0712	0.205	0.733
0.16	0.0712	0.116	0.517

Experimental Data for Fabric Number BR-18

∇P (inches water)	ρ ($lb_m - ft^{-3}$)	G ($lb_m - sec^{-1} - ft^{-2}$)	ψ ($lb_f Sec. ft^{-3}$)
High Pressure Apparatus:			
55	0.0759	2.69	7.66
50	0.0750	2.45	7.58
45	0.0742	2.28	7.31
40	0.0733	2.12	6.92
30	0.0717	1.79	6.09
21	0.0700	1.42	5.04
10	0.0683	0.986	3.60
4	0.0673	0.623	2.26
3	0.0672	0.542	1.95
2	0.0670	0.446	1.57
1	0.0668	0.331	1.06

Low Pressure Apparatus:

2.00	0.0712	0.388	1.94
1.60	0.0712	0.336	1.79
1.20	0.0712	0.275	1.64
0.80	0.0712	0.205	1.46
0.48	0.0712	0.125	1.44

Contrails
TABLE 14

Experimental Data for Fabric Number BR-30

γP (inches water)	ρ ($lb_m - ft^{-3}$)	G ($lb_m - sec^{-1} - ft^{-2}$)	ψ ($lb_f Sec. ft^{-3}$)
------------------------------	--------------------------------	--	-----------------------------------

High Pressure Apparatus:

22	0.0702	4.52	1.75
20	0.0699	4.32	1.66
17	0.0694	3.94	1.55
13	0.0687	3.42	1.36
10	0.0682	2.99	1.19
7	0.0677	2.48	1.01
5	0.0674	2.07	0.863
4	0.0672	1.84	0.755
3	0.0670	1.59	0.670
2	0.0669	1.32	0.530
1	0.0667	0.895	0.392

Low Pressure Apparatus:

0.35	0.0712	0.432	0.243
0.30	0.0712	0.400	0.226
0.20	0.0712	0.305	0.197
0.12	0.0712	0.220	0.164
0.064	0.0712	0.170	0.141

Experimental Data for Fabric Number BR-40

∇P (inches water)	ρ ($lb_m - ft^{-3}$)	G ($lb_m - sec^{-1} - ft^{-2}$)	ψ ($lb_f Sec. ft^{-3}$)
------------------------------	--------------------------------	--	-----------------------------------

High Pressure Apparatus:

55	0.0759	1.96	10.5
45	0.0742	1.74	9.55
35	0.0726	1.51	8.45
25	0.0709	1.26	7.14
20	0.0700	1.13	6.35
15	0.0692	0.955	5.61
10	0.0683	0.765	4.64
5	0.0675	0.543	3.24

Low Pressure Apparatus:

2.00	0.0712	0.360	2.09
1.60	0.0712	0.312	1.93
1.20	0.0712	0.354	1.78
0.80	0.0712	0.195	1.54
0.48	0.0712	0.152	1.19

TABLE 16

Experimental Data for 100 Mesh Wire Screen

∇P (inches water)	ρ ($lb_m - ft^{-3}$)	G ($lb_m \cdot sec^{-1} - ft^{-2}$)	ψ ($lb_f \cdot Sec. ft^{-3}$)
Large Orifices:			
8.45	0.0690	5.00	0.601
6.90	0.0688	4.56	0.536
5.75	0.0686	4.03	0.505
4.66	0.0685	3.64	0.452
3.48	0.0682	2.96	0.414
3.02	0.0681	2.79	0.381
2.27	0.0680	2.33	0.343
1.33	0.0678	1.73	0.271
0.646.	0.0677	1.12	0.203
Small Orifices:			
0.598	0.0676	1.06	0.200
0.533	0.0676	0.995	0.190
0.480	0.0676	0.915	0.186
0.410	0.0676	0.830	0.175
0.351	0.0676	0.755	0.165
0.273	0.0676	0.645	0.150
0.189	0.0676	0.500	0.134

Contrails

TABLE 17

Experimental Data for 150 Mesh Wire Screen

∇P (inches water)	ρ (lb _m - ft ⁻³)	G (lb _m - sec ⁻¹ - ft ⁻²)	ψ (lb _f Sec. ft ⁻³)
Large Orifice:			
6.11	0.0695	5.05	0.433
5.48	0.0693	4.72	0.415
5.01	0.0693	4.46	0.402
4.45	0.0692	4.16	0.382
3.92	0.0691	3.88	0.361
2.82	0.0689	3.22	0.313
2.14	0.0688	2.66	0.286
1.67	0.0687	2.30	0.258
1.10	0.0686	1.78	0.220
0.768	0.0686	1.43	0.191
Small Orifice:			
0.586	0.0669	1.17	0.175
0.516	0.0669	1.06	0.170
0.464	0.0669	0.990	0.164
0.410	0.0669	0.917	0.156
0.367	0.0669	0.850	0.151
0.301	0.0669	0.745	0.141
0.212	0.0669	0.574	0.129
0.178	0.0669	0.492	0.126

Contrails

TABLE 18

Experimental Data for 200 Mesh Wire Screen

∇P (inches water)	ρ ($lb_m - ft^{-3}$)	G ($lb_m - sec^{-1} - ft^{-2}$)	ψ ($lb_f Sec. ft^{-3}$)
Large Orifice:			
6.92	0.0702	5.00	0.502
5.85	0.0700	4.61	0.457
4.46	0.0698	3.97	0.405
3.33	0.0696	3.29	0.364
2.49	0.0695	2.70	0.332
2.04	0.0694	2.37	0.310
1.38	0.0693	1.84	0.270
0.790	0.0692	1.30	0.218
Small Orifice:			
0.686	0.0666	1.16	0.206
0.641	0.0666	1.12	0.200
0.563	0.0666	1.02	0.192
0.486	0.0666	0.920	0.184
0.391	0.0666	0.790	0.173
0.334	0.0666	0.700	0.166
0.267	0.0666	0.595	0.157
0.215	0.0666	0.494	0.152

Contrails

TABLE 19

Experimental Data for 270 Mesh Wire Screen

∇P (inches water)	ρ ($\text{lb}_m - \text{ft}^{-3}$)	G ($\text{lb}_m - \text{sec}^{-1} - \text{ft}^{-2}$)	ψ ($\text{lb}_f \text{ Sec. ft}^{-3}$)
Large Orifice:			
6.42	0.0707	5.05	0.460
5.42	0.0706	4.55	0.433
4.26	0.0703	3.93	0.394
3.13	0.0701	3.26	0.346
2.38	0.0700	2.67	0.323
1.73	0.0699	2.16	0.288
1.04	0.0698	1.52	0.247
0.362	0.0696	0.740	0.177
Small Orifice:			
0.701	0.0682	1.16	0.215
0.578	0.0680	1.00	0.205
0.474	0.0679	0.860	0.196
0.390	0.0677	0.745	0.186
0.308	0.0676	0.615	0.174
0.228	0.0674	0.486	0.166

Contrails

TABLE 20

α and β Values for Fabrics and Screens

Item Number	αL^* (10^6 ft. ⁻¹)	βL (ft. ^o)	α (10^9 ft. ⁻²)	β (10^3 ft. ⁻¹)	βL (10^{-6} ft.)
BR-1	0.565	18.8	1.99	66.2	33.2
BR-2	0.672	20.3	2.50	75.5	30.2
BR-5	0.550	16.5	1.65	49.5	30.0
BR-6	0.656	22.5	2.02	69.3	34.3
BR-9	0.552	16.9	1.83	56.2	30.2
BR-10	0.381	15.2	1.27	50.5	39.8
BR-11	0.540	17.5	1.58	51.0	32.3
BR-12	0.597	23.7	1.84	85.2	46.3
BR-13	0.921	44.8	2.70	131	48.5
BR-14	1.98	59.6	5.80	175	30.2
BR-17	1.38	35.4	4.15	106	25.6
BR-18	2.69	75.3	8.10	227	28.0
BR-30	0.211	11.9	4.22	238	56.4
BR-40	0.812	176	17.1	3700	217
100 mesh	0.203	3.54	2.55	42.5	17.4
150 mesh	0.227	2.30	1.65	16.0	10.0
200 mesh	0.260	2.78	1.58	16.0	10.7
270 mesh	0.314	2.41	1.28	9.2	7.70

Table 21. Physical Dimensions of Fabrics

Fabric Number	L (10^3 in)	S_w (10^{-3} in)	S_f (10^{-3} in)	d_w (10^{-3} in)	d_f (10^{-3} in)	ϵ (Dimensionless)	d_e (10^{-3} in)	ϵ (10^{-3} in)
BR-1	3.4	7.41	8.93	5.2	5.2	0.13	2.8	0.36
BR-2	3.3	7.35	8.33	5.2	5.2	0.11	2.6	0.29
BR-5	4.0	7.46	10.0	5.2	5.5	0.14	3.0	0.42
BR-6	3.9	7.30	9.26	5.2	5.5	0.12	2.7	0.32
BR-9	3.6	8.33	11.8	5.5	6.5	0.15	3.6	0.55
BR-10	3.6	8.47	12.2	5.5	6.5	0.16	3.9	0.65
BR-11	4.1	8.33	10.4	5.5	5.5	0.16	3.6	0.56
BR-12	3.9	8.26	9.35	5.5	5.5	0.14	3.3	0.47
BR-13	4.1	8.06	13.2	5.5	9.5	0.090	3.0	0.27
BR-14	4.1	8.06	11.4	5.5	9.5	0.054	2.2	0.12
BR-17	4.0	10.0	13.3	7.5	9.5	0.071	3.0	0.21
BR-18	4.0	9.71	11.4	7.5	9.5	0.038	2.0	0.078

TABLE 22

Physical Dimensions of Screens

<u>Mesh Number Per Inch</u>	<u>L (10⁻³ in)</u>	<u>S (10⁻³ in)</u>	<u>d (10⁻³ in)</u>	<u>ε dimensionless</u>	<u>d_e (10⁻³ in)</u>
100	10.0	10.0	4.5	0.302	5.5
150	5.8	6.7	2.6	0.373	4.1
200	4.8	5.0	2.1	0.337	2.9
270	3.2	3.8	1.6	0.305	2.1

SAMPLE CALCULATIONS

SAMPLE CALCULATIONS

Calculation of values of ∇P , ρ , G , and ψ .---The values of ∇P , ρ , G , and ψ given in Tables II through XIX were determined by a series of 23 operations which are described in the Master Data and Result Sheet (Figure 15). Of this list items 1 through 5 are self explanatory. The procedure of items 6 and 7 is used to find the correct value of ∇P^2 without excessive multiplication from the equation

$$\nabla P^2 = (2P_2 + P) \nabla P \quad (17)$$

This equation comes from the definitions of ∇P and ∇P^2 which are

$$\nabla P = P_1 - P_2 \quad (18)$$

and

$$\nabla P^2 = (P_1^2 - P_2^2) = (P_1 + P_2)(P_1 - P_2) \quad (19)$$

The combination of equations (18) and (19) results in equation (17).

Items 8 through 19 show the procedure of obtaining the rate of flow of air through the cloth from appropriate measurements of temperature and pressures using the general flow equation

$$M = CK \sqrt{\rho h_w} \quad (20)$$

where C is a constant containing the appropriate orifice and dimensional constants. In this procedure a trial value of the flow is first calculated using an assumed value for the orifice coefficient. The

Contrails

Reynolds number at the throat of the orifice is calculated and a corrected orifice coefficient obtained from a K versus N_{Re} curve appropriate to the orifice used. A typical orifice coefficient curve is shown in Figure 17. The correct flow is then calculated using the corrected orifice coefficient. The mass velocity is obtained in item 20 by dividing the mass flow by the area of the cloth exposed to the flow. In the operations indicated by items 21 through 23 the value of ψ is obtained from the definition

$$\psi = \frac{\nabla P^2}{2RTG} \quad (21)$$

Data pertinent to fabric BR-1 are used here as an example of the procedure used in taking the data and making the calculations. Figure 18 shows the log sheet on which the original data from the low pressure tunnel for sample number 1 were recorded; the plot of the orifice pressure drop versus static pressure in Figure 19 was made from this data. Table 23 illustrates the process used in obtaining average values of the orifice pressure drops for the nine samples. Table 24 shows in summary form the results calculated from the procedure indicated in the master data and result sheet.

Determination of the parameters α and β --- The parameters α and β are defined by the equation

$$\psi = \alpha L \frac{\mu}{g_c} + \frac{\beta L}{g_c} G \quad (22)$$

For convenience this equation may be written as

$$\psi = a + bG \quad (23)$$

Contrails

if

$$a = \alpha L \frac{\mu}{g_c} \quad (24)$$

and

$$b = \frac{\beta L}{g_c} \quad (25)$$

The constants a and b are determined by the method of averages, using the portion of the data which approximates a straight line on the graph. As an example of this method, the residual equations of Fabric BR-1 were grouped as follows:

$$\begin{array}{ll} a + 2.00 & b = 1.41 \\ a + 1.71 & b = 1.24 \\ a + 1.36 & b = 1.04 \\ a + 1.17 & b = 0.902 \\ a + 0.937 & b = 0.750 \\ a + 0.636 & b = 0.552 \end{array}$$

$$\begin{array}{ll} a + 0.435 & b = 0.484 \\ a + 0.348 & b = 0.432 \\ a + 0.300 & b = 0.402 \\ a + 0.250 & b = 0.360 \\ a + 0.195 & b = 0.308 \end{array}$$

$$6a + 7.813 \quad b = 0.894$$

$$5a + 1.528 \quad b = 1.986$$

The values of a and b are found by solving simultaneously the equations

$$6a + 7.813b = 5.894 \quad (26)$$

$$5a + 1.528b = 1.986 \quad (27)$$

The solutions of these equations give the values of a and b as

$$a = 0.216$$

$$b = 0.589$$

The values of αL and βL , which are given in Table 20, are obtained from equations (24) and (25). The value of the viscosity is taken from item 15, Table 20 and multiplied by a suitable factor to convert to consistent units.

Contrails

$$\alpha L = \frac{g_c}{\mu} a = \frac{32.2}{0.0185 \times 0.000672} \times 0.216 = 0.565 \times 10^6 \quad (\text{ft}^{-1})$$

$$\beta L = g_c b = 32.2 \times 0.589 = 18.8 \quad (\text{dimensionless})$$

The values of α and β are calculated from these values of αL and βL and the fabric thickness L given in Table 21.

$$\alpha = \frac{\alpha L}{L} = \frac{0.565 \times 12 \times 10^6}{3.4 \times 10^{-3}} = 1.99 \times 10^9 \quad (\text{ft}^{-2})$$

$$\beta = \frac{\beta L}{L} = \frac{18.8 \times 12}{3.4 \times 10^{-3}} = 66.2 \times 10^3 \quad (\text{ft}^{-1})$$

Calculation of plane porosity and effective diameter.---The thread dimensions for these sample calculations of ϵ and d_e for fabric BR-1 are taken from Table 21.

The plane porosity is defined as

$$\frac{\text{Projected free cell area}}{\text{Area of unit cell}} = \frac{(s_w - d_w)(s_f - d_f)}{s_w s_f}$$
$$\frac{(7.41 - 5.2)(8.93 - 5.2)}{7.41 \times 8.93} = 0.13$$

The effective diameter is defined as

$$d_e = \frac{4 \times \text{open cross-sectional cell area}}{\text{wetted perimeter of open area}}$$
$$= \frac{2 \times (s_w - d_w)(s_f - d_f)}{(s_w - d_w + s_f - d_f)}$$

Continued

$$\frac{2 \times (7.41 - 5.2)(8.93 - 5.2)}{(7.41 - 5.2) + (8.93 - 5.2)} \times 10^{-3}$$

$$= 2.8 \times 10^{-3} \text{ inches}$$

Contrails

<u>Item No.</u>	<u>Dimensions</u>
1. Barometer	in. hg.
2. Barometer, P_2 , (0.491 x item 1)	lb _f in ⁻²
3. Static pressure, ∇P	in. water
4. Static pressure, ∇P , (0.0362 x item 3)	lb _f in ⁻²
5. Static pressure, P , (item 2 + item 4)	lb _f in ⁻² abs.
6. $2P_a + \nabla P$, (2 x item 2 + item 4)	
7. ∇P^2 , (20,740 x item 6 x item 4)	lb _f ² ft ⁻⁴
8. Outlet air temperature, T	°F abs.
9. Orifice pressure drop, h_w	in. water
10. $2.71 \div T$, (2.71 ÷ item 7)	
11. Air density at cloth, ρ , (item 5 x item 10)	lb _m ft ⁻³
12. $h_w \rho$, (item 9 x item 11)	
13. $\sqrt{h_w \rho}$, (item 12) ^{1/2}	lb _m sec ⁻¹
14. Estimated air flow, M , (0.177 x item 13)	lb _m sec ⁻¹
15. Air viscosity, μ , (at temperature of item 8)	cp.
16. $\frac{M}{\mu}$ (item 14 ÷ item 15)	
17. Reynolds number at throat, N_{Re} , (13,780 x item 16)	
18. Corrected orifice coefficient, K	
19. Corrected flow, M_c , (item 14 x $\frac{\text{item 18}}{0.650}$)	lb _m sec ⁻¹
20. Mass velocity at cloth, G , (item 19 ÷ 0.20)	lb _m sec ⁻¹ ft ⁻²
21. $2RT$, (106.6 x item 8)	
22. $\frac{\nabla P^2}{G}$, (item 7 ÷ item 20)	
23. ψ , (item 22 ÷ item 21)	lb _f sec ft ⁻³

Figure 16. Master Data and Result Sheet

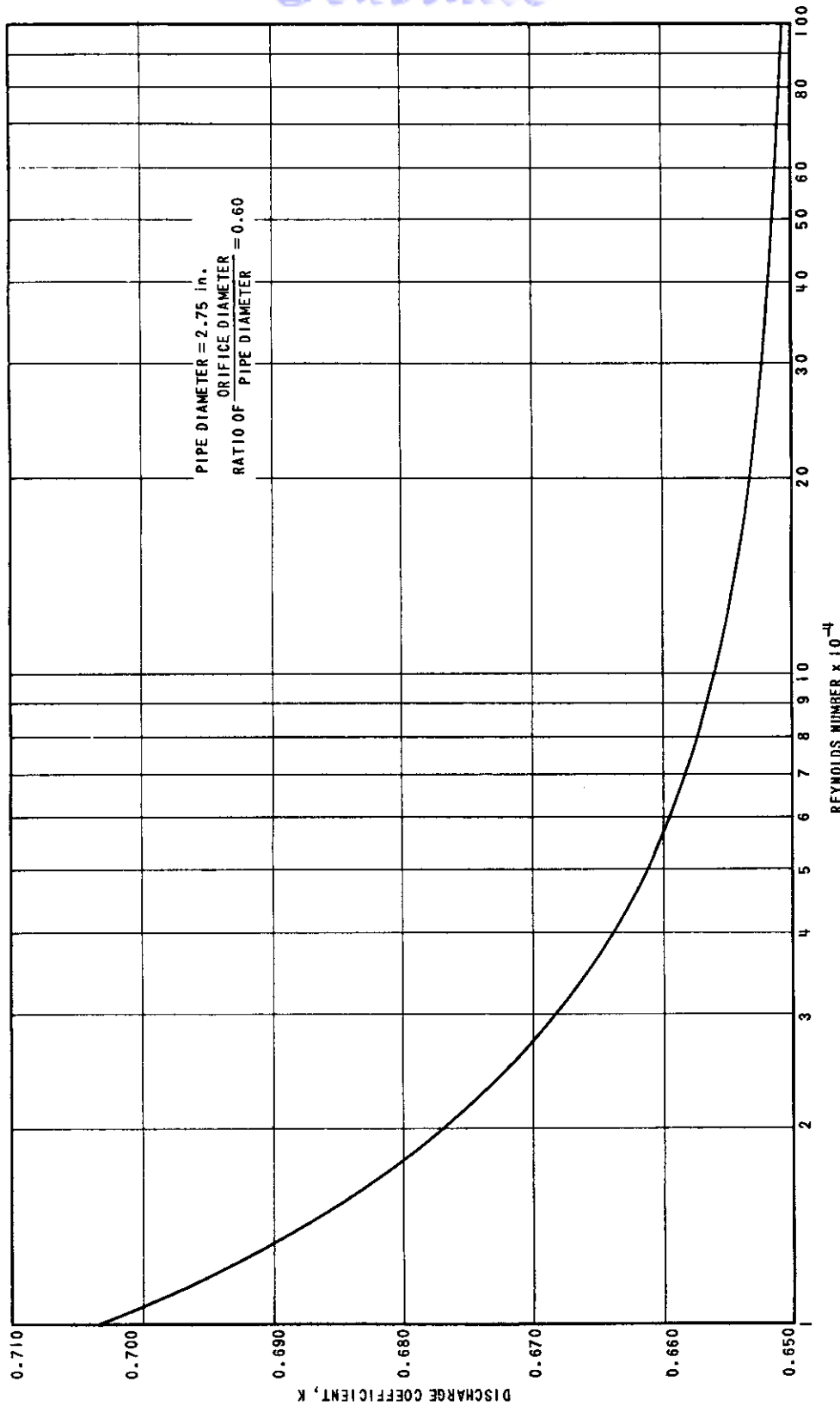


Figure 17. Orifice Coefficient Curve.

Centrails
LOG SHEET

Cloth Identification
Style No. 135 x 113
Fiber Content Nylon
Weave Pattern Plain
Color Style White

Run No. BR-1
Page No. 1

Remarks: Low Pressure Tunnel
Orifice ratio: 0.60
Baro. 29.25

<u>Test Number</u>	<u>Static Pressure in. Alcohol</u>	<u>Orifice Pressure Drop in. Alcohol</u>	<u>Temperatures °F.</u>	
			<u>Inlet</u>	<u>Outlet</u>
Zero Readings	0.00	0.00		
1	0.114	0.364	79	83
2	0.220	0.983	79	83
3	0.421	2.342	79	83
4	0.568	3.472	79	83
5	0.665	4.360	79	83

Figure 18. Sample Log Sheet

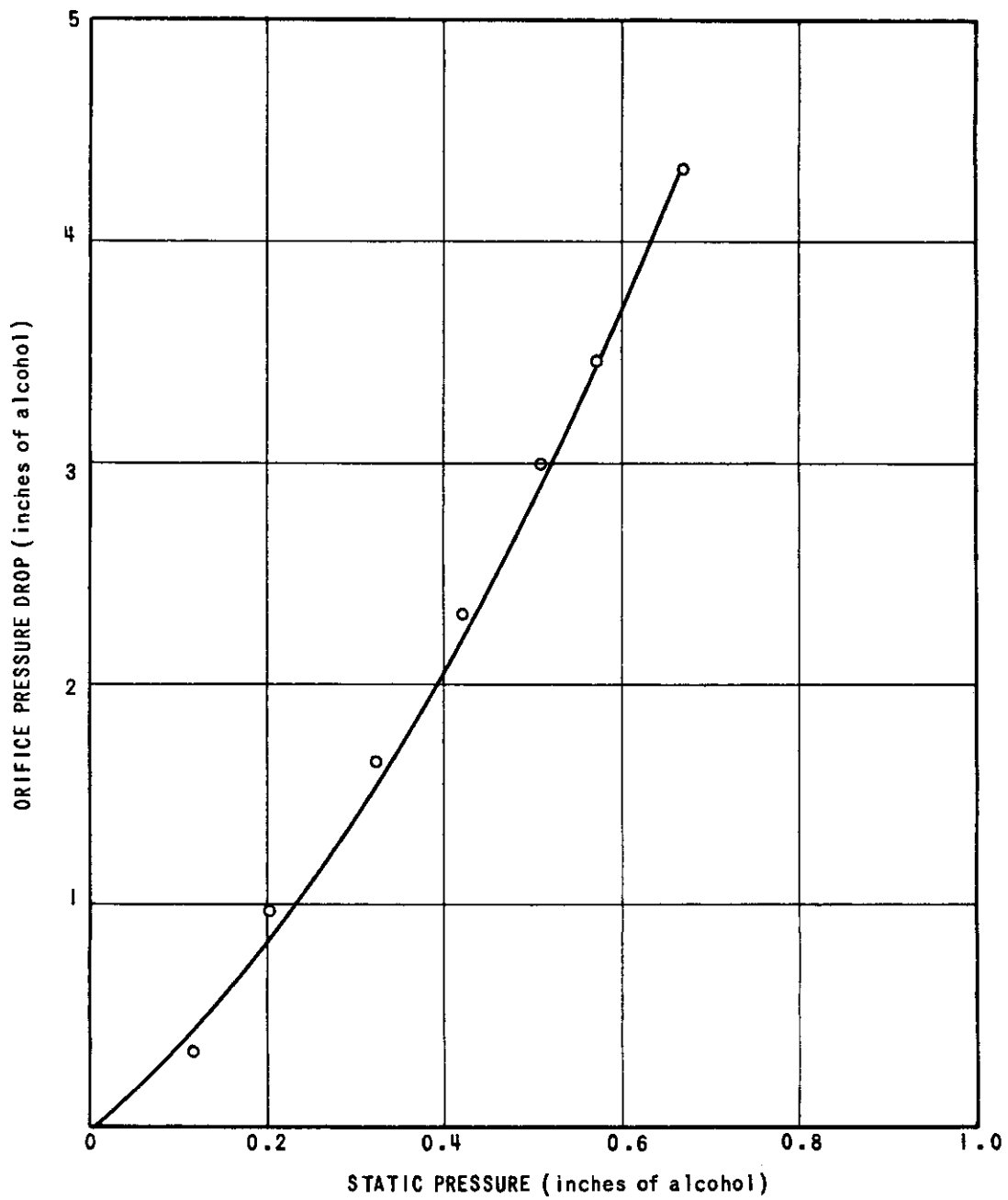


Figure 19. Relation of Static Pressure to Orifice Pressure Drop.

Contrails

Table 23. Data on Averaged Orifice Pressure Drop Vs Static Pressure

Cloth Identification
 Style No. 135 x 113
 Fiber Content Nylon
 Weave Pattern Plain
 Color Style White

Ref: Log Sheet
 Run No. BR-1
 Page No. I

	<u>Orifice Pressure (inches of alcohol)</u>				
<u>∇P</u> <u>(in. water)</u>	<u>0.16</u>	<u>0.24</u>	<u>0.32</u>	<u>0.40</u>	<u>0.56</u>
1	0.80	1.42	2.22	2.90	4.70
2	0.78	1.32	2.00	2.70	4.40
3	0.60	1.08	1.70	2.32	4.00
4	0.83	1.40	2.00	2.72	4.38
5	0.65	1.12	1.70	2.30	3.97
6	0.60	1.10	1.72	2.32	4.00
7	0.67	1.10	1.60	2.15	3.50
8	0.71	1.22	1.80	2.50	4.05
9	<u>0.67</u>	<u>1.13</u>	<u>1.68</u>	<u>2.25</u>	<u>3.85</u>
Ave.	0.70	1.21	1.82	2.46	4.09
Corrected h_w (In. water)	0.56	0.97	1.46	1.97	3.27

Contrails

Table 24. Sample Data and Result Sheet

Cloth Identification

Style No. 135 x 113
Fiber Content Nylon
Weave Pattern Plain
Color Style White

Ref: Log Sheet

Run No. BR-1

Page No. 1 to 9

<u>Item Number</u>	<u>Test Number</u>				
1	29.25	29.25	29.25	29.25	29.25
2	14.35	14.35	14.35	14.35	14.35
3	0.16	0.24	0.32	0.40	0.56
4	0.0058	0.0087	0.0115	0.0145	0.0202
5	14.36	14.36	14.36	14.36	14.37
6	28.70	28.71	28.71	28.71	28.72
7	3450	5180	6850	8630	12,000
8	543	543	543	543	543
9	0.56	0.97	1.46	1.97	3.27
10	0.00498	0.00498	0.00498	0.00498	0.00498
11	0.0715	0.0715	0.0715	0.0715	0.0715
12	0.0402	0.0695	0.105	0.141	0.235
13	0.201	0.264	0.324	0.377	0.485
14	0.0356	0.0467	0.0574	0.0667	0.0858
15	0.0185	0.0185	0.0185	0.0185	0.0185
16	1.92	2.52	3.10	3.60	4.63
17	26,500	34,800	42,800	49,700	63,800
18	0.670	0.666	0.663	0.661	0.658
19	0.0367	0.0477	0.0585	0.0677	0.0870
20	0.184	0.238	0.292	0.338	0.435
21	57,900	57,900	57,900	57,900	57,900
22	18,800	21,700	23,500	25,500	27,600
23	0.324	0.375	0.407	0.443	0.478

NOMENCLATURE

A	Area
a	Viscous Coefficient
b	Inertial Coefficient
C_d	Drag Coefficient
C_f	Flow-Through-Resistance Coefficient
d_e	Effective Diameter
d_w	Width of Warp Threads
d_f	Width of Filling Threads
G	Mass Velocity
g_c	Dimensional Constant
h	Head of Fluid Across Orifice
K	Orifice Discharge Coefficient
L	Thickness of Fabric
M	Mass Flow
N_{Re}	Reynolds Number
P	Pressure
Q	Volume Rate of Flow
R	Gas Constant
s_w	Spacing of Warp Threads
s_f	Spacing of Filling Threads
T	Temperature
v	Velocity

- α Viscous Parameter
- β Inertial Parameter
- ∇P Pressure Differential
- ∇P^2 Pressure-Squared Differential
- ϵ Plane Porosity
- μ Viscosity
- ρ Density
- ϕ Solidity
- $\psi = \frac{\nabla P^2}{2RTG}$
- 1 Upstream of Cloth
- 2 Downstream of Cloth

1. Goglia, M. J., Air Permeability of Parachute Cloths. Tech. Rep. No. 1, Proj. 170-117, G.I.T., Atlanta, Ga., pp. 9-10. (1952)
2. Schiefer, H. F. and Paul M. Boyland, "Improved Instruments for Measuring the Air Permeability of Fabrics", Nat. Bur. of Stda. J. Res. 28, 637-642 (May 1942).
3. Penner, Stuart E., A Study of Flow Through Fabric-Like Structures. Unpublished M. S. Thesis, Inst. of Text. Tech., Charlottesville, Va., 1950.
4. Backer, Stanley, "The Relation Between the Structural Geometry of a Textile Fabric and Its Physical Properties", Part IV., Text. Res. J. 10, 703-114, (1951).
5. Rainard, L. W., "Air Permeability of Fabrics I.", Text. Res. J. 16, 473-80, (1946).
6. Robertson, A. F., "Air Porosity of Open Weave Fabrics", Text. Res. J. 20, 838-57, (1950).
7. Backer, op. cit.
8. Robertson, A. F., Air Permeability of Parachute Fabrics. Status Rep., Proj. 5007, Inst. of Text. Tech., Charlottesville, W. Va., (June 1949).
9. Landsberg, M. I. and Gerald Winston, Relationship Between Measurements of Air Permeability of Two Machines. Pub. Board 97014, (Q. M. C. TSR 35).
10. Goglia, op. cit., pp. 68-71.
11. Green, Leon and Pol Duwez, "Fluid Flow Through Porous Media", J. of App. Mech. 18, No. 1., 39-45, (1951).
12. Fluid Meters Report, 4th ed., Am. Soc. Mech. Engrs., New York, 1947.
13. Glaskin, A., A Statistical Note on the Variation of Porosity of Nylon Fabric to Specification D. T. D. 556 A., E & M 2213, Brit. Min. of Supply, A. R. C., TN, (June 1945).
14. Modern Developments in Fluid Dynamics, edited by Sydney Goldstein, Vol. II, Oxfor, University Press, New York, 1938. pp. 418-19.

15. Goglia, op. cit., p. 127.
16. Hoerner, S. F., Pressure Losses Across Screens and Grids. AF Tech. Rept., No. 6289, (nov. 1950).